Assessing the diversity of plankton-associated prokaryotes along a size-fraction gradient: A methodological evaluation

Léa Cabrol, Mélanie Delleuze, Arthur Szylit, Guillaume Schwob, Marianne Quemeneur, Benjamin Misson

Assessing the diversity of plankton-associated prokaryotes along a size-fraction gradient: a methodological evaluation

Marine Pollution Bulletin, Volume 197, December 2023, 115688

https://doi.org/10.1016/j.marpolbul.2023.115688

Authors :

Léa Cabrol[a,b,c], Mélanie Delleuze[b,d], Arthur Szylit[c], Guillaume Schwob[b,d], Marianne Quéméneur[a], Benjamin Misson[e]

Authors affiliations:

a Aix Marseille Univ, Université de Toulon, CNRS, IRD, MIO, Marseille, France

b. Millennium Institute BASE "Biodiversity of Antarctic and Subantarctic Ecosystems", Las Palmeras 3425, Santiago, Chile

c. Instituto de Ecologia y Biodiversidad, Santiago, Chile

d. Departamento de Ciencias Ecológicas, Facultad de Ciencias, Universidad de Chile, Santiago, Chile

e. Université de Toulon, Aix Marseille Univ., CNRS, IRD, MIO, Toulon, France

Corresponding author:

Léa Cabrol, lea.cabrol@mio.osuptheas.fr , Aix Marseille Univ, Universit´e de Toulon, CNRS, IRD, MIO, Marseille, France.

Received 10 February 2023; Received in revised form 29 September 2023; Accepted 16 October 2023
Available online 27 October 2023

Keywords: plankton size fraction; DNA extraction method; cell desorption; prokaryotic DNA enrichment; Vibrio; eukaryotic DNA depletion

Highlights:

- The plankton microbiota differed strongly according to the plankton size-fraction.
- The bulk community (> 0.2 µm) was more similar to the 0.2-90 µm fraction.
- Cell desorption pretreatment led to a biased over-representation of *Vibrionaceae*.
- The influence of prokaryotic DNA enrichment was taxon-specific.

Graphical abstract:

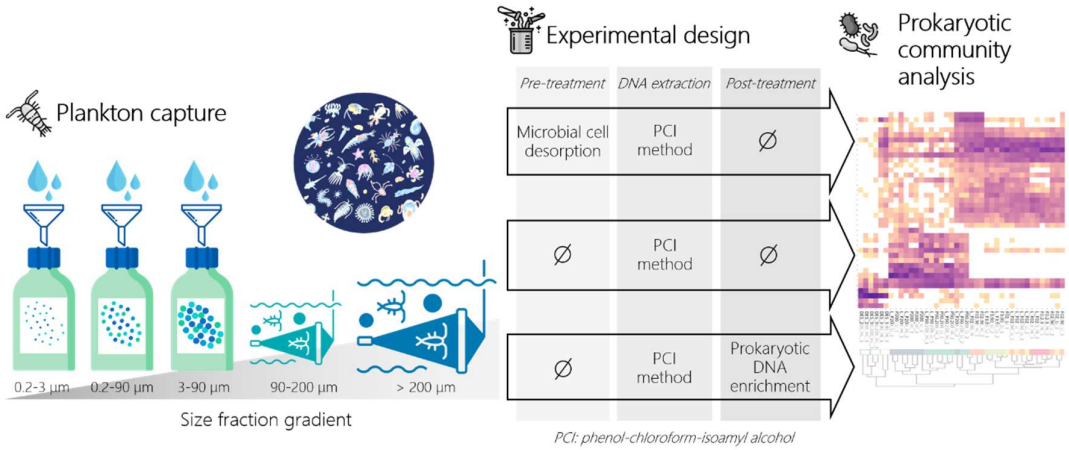

Abstract

Marine free-living (FL) and plankton-associated prokaryotes (plankton-microbiota) are at the basis of trophic webs and play crucial roles in the transfer and cycling of nutrients, organic matter, and contaminants. Different ecological niches exist along the plankton size fraction gradient. Despite its relevant ecological role, the plankton-microbiota has rarely been investigated with a sufficient level of size-fraction resolution, and it can be challenging to study because of overwhelming eukaryotic DNA. Here we compared the prokaryotic diversity obtained by 16S rRNA gene sequencing from six plankton size fractions (from FL to mesoplankton), through three DNA recovery methods: direct extraction, desorption pretreatment, enrichment post-treatment. The plankton microbiota differed strongly according to the plankton size-fraction and methodological approach. Prokaryotic taxa specific to each size fraction, and methodology used, were identified. *Vibrionaceae* were over-represented by cell desorption pretreatment, while prokaryotic DNA enrichment had taxon-specific effects, indicating that direct DNA extraction was the most appropriate method.

Introduction

At the basis of marine trophic webs, plankton is classically divided into phytoplankton (unicellular photosynthetic autotrophs) and zooplankton (protists and metazoan animals). Phytoplankton size ranges from 0.2-3 µm (picophytoplankton), to 3-25 µm (nanophytoplankton), and 25-200 µm (microphytoplankton), while the best known and studied fraction of zooplankton is larger than 200 µm (D'Alelio et al., 2019; Sieburth, John McN; Jürgen Lenz, 1978). In addition, a major biological compartment in marine ecosystems is constituted by prokaryotes, which can have a free-living (FL, usually in the range 0.2-1~5 µm) or particle-attached (PA, > 1~5 µm) lifestyle (Michotey et al., 2012; Rieck et al., 2015; Smith et al., 2013; Yung et al., 2016). There is no clear size consensus to define each category, the 1-5 µm fraction being usually considered as 'ambiguous' (Yung et al., 2016).

The plankton-associated prokaryotes (plankton-microbiota) play a crucial role in the exchange and cycling of nutrients, organic matter, organic and inorganic contaminants (especially trace metals, PCBs, HAPs, microplastics) at the oceanic ecosystem scale (Chouvelon et al., 2019; Pouch et al., 2022; Rodrigues et al., 2021). The plankton-microbiota either prevents or favors the entrance of contaminants in the first compartments of the trophic web, through passive (e.g. sorption) or active (e.g. redox) mechanisms. The plankton-microbiota can also impact human and marine life health through the development and transport of pathogens (Maugeri et al., 2004). The sinking particles are considered as vectors for the vertical connectivity of microbial communities in the water column from the surface down to the deep sea (Mestre et al., 2018; Puigcorbé et al., 2023).

The local environmental conditions can drastically differ between the particles microenvironment (i.e. PA habitat) and the surrounding water (FL habitat), resulting for instance in strong oxygen or nutrient gradients. Consequently, there is a strong niche partitioning between PA and FL communities, leading to different microbial structures and functions (Yeh & Fuhrman, 2022). Different environmental factors affect the FL and PA microbial communities (Roth Rosenberg et al., 2021). While FL and PA communities have often been compared (e.g. (Ghiglione et al., 2009; Rieck et al., 2015)), the nature of PA habitat is generally not taken into consideration in PA community variability. The particle size and nature might play an important role in structuring PA communities. The structural and metabolic diversity of pico-, nano-, micro-phytoplankton and zooplankton (e.g. in terms of exudate composition, or cell wall characteristics) are expected to create different host-associated microhabitats along the plankton size gradient, thus selecting for size-specific microbial assemblages. As such, the characteristics of the particle microhabitat can overwhelm the bulk seawater environmental drivers in shaping PA microbial community structure (Yung et al., 2016). Yet,

little attention has been paid to marine plankton-microbiota, especially in large size fractions, despite their quantitative importance and relevant ecological role.

The plankton-microbiota is challenging to study. Direct DNA extraction from prokaryotic/eukaryotic assemblages may lead to overwhelming amounts of host DNA, limiting the recovery of satisfying prokaryotic DNA amounts for subsequent molecular analysis. Different procedures have been proposed to separate microbiota from host, either before DNA extraction (i.e. through desorption of the surface microbiota), or after DNA extraction (i.e. through specific enrichment of prokaryotic DNA). Desorption methods have been widely used on different types of matrices such as sediment, algae, woodchips (e.g. (Cabrol et al., 2010; Michotey et al., 2020)). Several prokaryotic DNA enrichment methods are based on the different characteristics of epigenetic DNA methylation between prokaryotes (low level of methylation, mainly on adenine) and eukaryotes (high level of methylation, mainly on cytosine in CpG patterns) (Shi et al., 2022). Beyond the mostly studied animals and plants, CpG methylation does also occur in microeukaryotic phytoplankton (Tirichine et al., 2017) such as marine diatoms (Hoguin et al., 2023; Traller et al., 2016; Veluchamy et al., 2013), dinoflagellates (De Mendoza et al., 2018), kelp (Fan et al., 2020), and marine zooplankton such as copepods (Aluru et al., 2021) or pteropod (Bogan et al., 2020). Enrichment of small quantities of bacterial DNA from a predominantly eukaryotic DNA extract is possible through the specific affinity of certain proteins for non-methylated (prokaryotic) CpG dinucleotides, as proposed by the Looxster enrichment kit, which showed high yield and sensitivity for prokaryotic DNA (Wiesinger-Mayr et al., 2011) and successfully enabled to detect previously undetected microbial genera (Glassing et al., 2015). A similar approach, relying on the selective binding and removal of CpG-methylated host-DNA, has been used for metagenomics of different host-microbiotas (Rubiola et al., 2020; Wagner Mackenzie et al., 2018). Other enrichment methods are based on a differential lysis of host cells, followed by DNAse degradation of the released extracellular DNA, but they require intact fresh (living) cells (Shi et al., 2022). These indirect DNA recovery methods, including pretreatment (desorption) and/or post-treatment (enrichment), might induce a bias in the representation of microbial community structure compared to direct DNA extraction. Moreover, the efficiency, representativeness and reliability of these methods are likely to be sample-dependent and might be influenced by the targeted planktonic size-fraction.

Considering the need to better characterize plankton-associated bacteria while minimizing methodological biases, and recognizing the possible cross-effects between extraction method and planktonic size fraction, the objective of this study was to compare the prokaryotic diversity obtained through different DNA recovery methods from different plankton size classes. For this purpose, three DNA recovery methods, either direct or indirect (desorption pretreatment, enrichment post-

119 treatment), followed by 16S rRNA gene sequence analyses, were evaluated on six plankton size
120 fractions (ranging from FL prokaryotes to mesoplankton microbiota). This methodological evaluation
121 will serve as a preliminary study to set up the DNA extraction method to be used in the MERITE-
122 HIPPOCAMPE campaign across the Mediterranean sea (Tedetti et al., 2023).

123

124 Material and Methods

125 Experimental design

126 The prokaryotic communities from 6 planktonic size fractions (> 0.2 µm, 0.2–3 µm, 0.2-90 µm, 3-90
127 µm, 90-200 µm, > 200 µm) were characterized and compared, using three different DNA recovery
128 methods: (i) direct DNA extraction, (ii) cell desorption pretreatment, (iii) prokaryotic DNA enrichment
129 post-treatment. Two input amounts of raw material for DNA extraction were tested on three size
130 fractions (0.2-90 µm, 90-200 µm, >200 µm). Depending on the considered plankton size fraction, the
131 potential risk of eukaryotic contamination differed, resulting in the choice of different methods
132 combinations (Table 1). The resulting 21 experimental conditions were carried out on biological
133 duplicates (n = 42).

134 The 0.2-3 µm fraction corresponds to heterotrophic bacteria and archaea, and autotrophic prokaryotes
135 (e.g. Cyanobacteria) and eukaryotes (e.g. Bathycoccus) (Sieburth et al., 1978) . The fraction below 90
136 µm encompasses most dinoflagellates (e.g. Alexandrium, Dinophysis, Oxyphysis, Gymnodinium),
137 silicoflagellates (e.g. Dictyocha) and flagellates (e.g. Ebria), with highly variable shapes, as well as some
138 small single-celled diatoms such as the centric Actinoptychus or Odontella (Horner, 2002). Above 90
139 µm, are found some large single-celled diatoms (such as the centric discoid shaped Asteromphalus or
140 the pennate shaped Navicula), and most usually chains of diatoms (Göröcs et al., 2018). Individually,
141 chain-forming diatoms can be smaller than 90 µm (such as the centric shaped Leptocylindrus,
142 Skeletonema, or Chaetoceros) or larger (such as the centric shaped Cerataulina or Eucampia, that form
143 straight and helical chains, respectively; or the pennate shaped Asterionellopsis or Thalassionema, that
144 form star like and zigzag chains, respectively), and they all assemble in chains that usually exceed 90
145 µm (Siokou-Frangou et al., 2010). Copepod nauplii, ciliates (e.g. tintinnids), and some dinoflagellates
146 (e.g. Ceratium, Protoperidium, or small chains of Alexandrium cells) are also usually in the 90-200 µm
147 fraction. Finally, the fraction larger than 200 µm represents the micro zooplankton class (e.g. copepods
148 and other micro crustaceans), and also includes some large dinoflagellates (e.g. Noctiluca), large single-
149 celled diatoms (such as Coscinodiscus or Rhizosolenia) , and invertebrate larva.

150 Sampling

All samples were collected in Toulon bay, Mediterranean Sea, France (43.1101581 N, 5.9265068 E) on the 30th of May 2018. For obtaining plankton size fractions <90 µm, surface seawater samples were collected with a 4.2L van Dorn bottle (Wildco) at 0.5 m-depth and transferred to 25L cans, kept at 4°C until further filtration at the laboratory, up to 6 h after sampling.

Size fractionation

All filtrations were performed on 47 mm-diameter cellulose ester filters (Millipore, Merck) of different porosities (0.22 or 3 µm) with a vacuum pump. Direct filtrations were carried out on raw seawater, while sequential filtrations were carried out after pre-filtration on 3 µm-cellulose filter or 90 µm-nylon mesh. All filtered volumes are indicated in Supplementary Table S1. For the 0.2-90 µm fraction, we compared two filtration volumes: 2.5 L ('low input', Li) and 4L ('high input', Hi). All filtrations were carried out under sterile conditions in laminar flow hood using autoclaved recipients. The filters were stored at -20°C until extraction.

Larger plankton size fractions were collected by horizontal sub-surface transects using Apstein plankton nets with of 90- or 200-µm mesh width, equipped with a digital flow meter. Each transect allowed to collect plankton from 19 and 84,5 m^3 of seawater for the 90- and 200-µm nets, respectively. To recover specifically the 90-200 µm fraction, the raw 90 µm fraction was washed with sterile NaCl solution (38 g L^{-1}) and filtered on 200 µm nylon mesh, three times. The mass of recovered plankton was 13.6 g for the > 200 µm fraction, and 9.7 g for the 90-200 µm fraction. Aliquots of raw plankton were stored at -20°C until further processing (either direct DNA extraction or desorption).

Cell desorption

Three different size classes were subjected to desorption, using as matrix either filters (for the 3-90 µm fraction) or raw plankton (for the 90-200 and > 200 µm fractions). The mass of raw plankton used for desorption was 2.5 and 3.5 g per replicate for the 90-200 and > 200 µm fractions, respectively. The corresponding seawater volumes are indicated in Supplementary Table S1. Up to 2h after sampling and filtration, the raw plankton matrix was resuspended at a 1:5 w/v ratio in a sterile desorption buffer (composition given in Supplementary Material). The filter matrix was resuspended in 12 mL of the same buffer. The mixtures were shaken on horizontal agitator (80 rpm) at 4°C for 1h. During that time, the tubes containing the mixtures where subjected to three sonication cycles (1 min each 20 min) in a ultra-wave bath (40kHz, Ultrasonic Cleaner 200, Branson), as adapted from Michotey *et al.* (Michotey et al., 2020).

After the agitation-sonication, the liquid phase was filtered under laminar flow hood, on a 3 µm, 90 µm or 200 µm membrane for, respectively, the 3-90, the 90-200 and the >200 µm fractions. The

183 filters were washed with sterile NaCl solution (38 g L^{-1}) and exposed to an additional cycle of
184 agitation-sonication. The filtrates from both steps were pooled, and microbial communities were
185 retrieved as follows. For the 3-90 µm fraction, the combined filtrate was further filtered on 0.22 µm
186 filter for subsequent DNA extraction. For the 90-200 and the >200 µm fractions, the combined
187 filtrate was centrifuged for 20 min at 10,000 g and 5°C due to filtration clogging, and the pellet was
188 stored at -20°C for subsequent DNA extraction.

189

190 **DNA extraction**

191 Total DNA was extracted from all samples by phenol-chloroform-isoamyl alcohol method, as detailed
192 in Supplementary material. For the 90-200 and >200 µm raw plankton (without desorption), two
193 masses of plankton were tested as template for DNA extraction: 0.25 g ('low input', Li), and 1 g ('high
194 input', Hi). The corresponding filtered water volumes to obtain these plankton masses are indicated
195 in Supplementary Table S1. DNA concentration and quality were checked by absorbance
196 (BioSpecnano spectrophotometer, Shimadzu).

197 **Enrichment of prokaryotic DNA**.

198 DNA extracts were divided in two subsamples: one for direct use for diversity analysis; one for
199 further prokaryotic enrichment with the Looxster Enrichment kit (Analytik Jena, Germany) to remove
200 the eukaryotic DNA, following the manufacturer's instructions. The Looxster enrichment method
201 uses of a derivative of human CXXC finger protein with a specific affinity to non-methylated CpG
202 dinucleotides. The Looxster protein, attached on magnetic particles, forms a stable complex with
203 non-methylated CpG-dinucleotides (prokaryotic DNA), which is recovered by a magnetic separator.
204 Unbound methylated DNA (eukaryotic) is removed from the sample by means of stringent washing
205 step.

206 **Microbial diversity and community structure**.

207 The V4-V5 region of 16S rRNA genes of Bacteria and Archaea was amplified by PCR with the 515F
208 (GTGYCAGCMGCCGCGGTA)-928R (CCCCGYCAATTCMTTTRAGT) primer set (Wang & Qian, 2009), using
209 GoTaq Long Master Mix (Promega). The PCR program was: 2' at 95°C; 30 cycles at 95°C for 30", 50°C
210 for 45" and 72° C for 45"; 10' at 72°C. After quantity and quality check on agarose gel electrophoresis,
211 the PCR products were sequenced on a MiSeq Illumina platform (Genotoul, Toulouse) producing 2 x
212 250 bp paired-end reads. Raw sequence reads have been deposited on the Sequence Read Archive

(SRA) of the NCBI GenBank, under the accession numbers SAMN32961579 to SAMN32961619, Bioproject number PRJNA929516.

Bioinformatic analysis.

The 2,185,748 raw sequences were processed with the FROGS pipeline version 3.2.3 on the Galaxy platform as previously described (Lavergne et al., 2021) (details provided in Supplementary Material). After filtration at 0.005% abundance threshold, 813,230 sequences were obtained and clustered in 971 OTUs, as defined by Swarm clustering. The numbers of sequences and OTUs after each treatment step are provided in Supplementary Table S2 for each sample type. Taxonomic affiliation was performed against SILVA 16s rRNA database (v138.1).

The output BIOM was analyzed in R (v4.1.1), mainly using the *phyloseq* package (v1.38.0). The chloroplast sequences (representing on average 2.1 % of the communities) were removed from the dataset). The OTU count table was rarefied to the lowest number of reads per sample (i.e. 2189 sequences). Alpha diversity was estimated using the Shannon index. The effects of size class, input amounts, enrichment treatment, and desorption step on the diversity were evaluated using pairwise Wilcoxon signed-rank test (with Holm adjustment).

The community composition variations were explored by principal coordinate analysis (PCoA, *ordinate* function) calculated from Bray-Curtis dissimilarity. The contribution of DNA recovery method and planktonic size fraction on community variation was tested by non-parametric permutational multivariate analysis of variance (PERMANOVA) using Bray Curtis distance with the *adonis2* function (*vegan* package, v2.5.7). To evaluate the effect of a single factor within specific treatment blocks, nested PERMANOVA was applied with the 'strata' parameter. The pairwise differences between size fractions were tested with the *pairwise.adonis* function (*funfun* package). The interacting effect of Looxster treatment and size fraction was evaluated for specific taxa by ANOVA and Tukey post-hoc test (*aov* and *TukeyHSD* functions). The top 10 most discriminating OTUs driving the community differentiation according to each size fraction and DNA recovery method were identified by two linear discriminant analysis (LDA) with the *run_lefse* function (*microbiomeMarker* package v0.99.0, with multigrp_strat = FALSE), resulting in 72 unique OTUs (100 permutations, p-value < 0.05). The 72 OTUs were aggregated at the last available taxonomic rank, resulting in 45 taxa. After removing the 5 least abundant taxa (i.e. < 6% on the sum of samples, approximately 0.1% per sample) ,the log-transformed relative abundances of these 40 discriminant taxa across the 41 samples were visualized on a heatmap (*plot_heatmap* function, *phyloseq* package). Taxa and samples were hierarchically clustered on the basis of their differential abundance patterns, using the Bray-Curtis distance and the ward.D2 method for dendrogram representation. To further investigate the microbial taxa that exhibited specific enrichments within each size fraction individually, we conducted pairwise Linear Discriminant Analysis

Effect Size (LEfSe) comparisons between the bulk and each one of the other fractions, using the default parameters of the run_lefse function and the maximum numbers of boostrap allowed by each size fraction dataset.

Results

Desorption pretreatment induced a loss of alpha diversity

The DNA recovery method had a significant effect on Shannon diversity index (Figure 1A). The desorption pre-treatment led to significantly lower diversity compared to direct extraction and subsequent Looxster enrichment (pairwise Wilcoxon tests, *p*-values < 0.005).

When considering only the subset of samples without desorption pretreatment, there was a significant effect of planktonic size fraction on Shannon diversity index (Kruskal-Wallis test, *p*-value < 0.01). Specifically, the 90-200 µm fraction community exhibited a significantly higher diversity than the 0.22-3 and 0.22-90 µm communities (pairwise Wilcoxon test, *p*-values < 0.05) (Figure 1A). Direct extraction and subsequent Looxster enrichment yielded statistically similar diversity, independently of the size fraction (*p*-values > 0.25). The three conditions that compared low and high inputs for DNA extraction did not lead to significantly different Shannon diversity indexes (Kruskal-Wallis test, *p*-value=0.36) (Supplementary Table S3). Nevertheless these non-significant results might be due to the low number of replicates.

Major effects of planktonic size-fraction and desorption pretreatment on prokaryotic community structure

We observed a strong effect of the planktonic size fraction along the first axis (40 % of the variance) of the PCoA ordination (PERMANOVA, *p*-value<0.001, R^2= 0.46) (Figure 1B) and microbial community structure first clustered by size (Figure 1C). The microbial community structures within the small and intermediate size fractions (> 0.22 µm, 0.22-3 µm, 0.22-90 µm) were not significantly different (PERMANOVA, *p*-values > 0.1). More specifically, the Bray-Curtis distance-based dendrogram shows that the bulk (> 0.22 µm) community clustered more tightly with the low-input 0.22-90 µm community (Figure 1A), both obtained from the same volume (2.5 L) of filtered seawater. The bulk community exhibited the highest variability among replicates (Bray-Curtis dissimilarity 0.28 ± 0.03), while the 0.22-90 µm fraction led to more stable communities between replicates (Bray-Curtis dissimilarity 0.17 ± 0.03). For the high filtered volumes (Hi, 4 L), the 0.22-90 µm fraction clustered together with larger fraction (90-200 µm) suggesting that during this prolonged filtration some larger particles could have passed through the filter.

Without considering the desorbed samples, the 3-90 µm fraction was significantly different from the 0.2-3 and 0.2-90 µm fractions (p values 0.032 and 0.042, respectively), but not from the > 0.2 µm fraction, suggesting that the bulk community contains some larger particles. The strongest community differences were observed between the four smallest and the two largest size fractions (PERMANOVA, *p*-values < 0.02). Within the large size fractions, significant differences in microbial community structure were also detected between the not-desorbed 90-200 µm and >200 µm fractions (PERMANOVA, *p*-value 0.015, Supplementary Figure S1). Within not-desorbed samples, no significant effect of the raw material amount was detected on microbial community structure (PERMANOVA, *p*-values > 0.2).

The second major driver of community structure was the desorption pretreatment (PERMANOVA, *p*-value < 0.001, R^2= 0.17), that discriminated the samples along to the second PCoA axis (about 19 % of the variance, Figure 1B). The desorbed communities clearly differed according to the size fraction (*i.e.* 3-90 µm vs larger fractions), however the experimental design did not allow to test for statistical differences between the desorbed 90-200 µm and > 200 µm fractions.

Different taxonomic indicators along the planktonic size gradient

The small size-fraction microbiota (0.22 µm, 0.22-3 µm and 0.22-90 µm) was dominated by Proteobacteria and Bacteroidota phyla, representing 65.8 ± 6.2 % and 22.6 ± 2.2 % of the community respectively (Figure 1C). Within Proteobacteria, the most discriminant taxa of the three small size-fractions were affiliated to Alphaproteobacteria from the SAR11 clade (17.9 ± 9.4 % of the community) and *Rhodobacteraceae* (15.4 ± 4.7 %), followed by *Halieaceae* (8.2 ± 3.3 %) in the Gammaproteobacteria class (Figure 2, Figure 3). Within Bacteroidota, the most discriminant taxa of the three small size-fraction microbiota were *Flavobacteriaceae* (14.8 ± 3.3 % of the community) and *Balneola* (5.4 ± 2.3 %) (Figure 2, Figure 3). Interestingly, different microbial taxa exhibited specific enrichment within each small size fraction individually, as shown by pairwise LEfSe comparisons between the bulk and each one of the other fractions (Supplementary Figure S2). Compared to the two other small fractions (0.22-3 and 0.22-90 µm), the bulk fraction was enriched in specific *Flavobacteriaceae* OTUs (distinct from the *Flavobacteriaceae* OTUs enriched in the other small fractions), Cyanobacteria, and *Halieaceae*, while it was deprived of *Ca*. Aquiluna (specific of 0.22-3 µm fraction) and *(Pseudo)alteromonas* (specific of the 0.22-90 µm fraction), among others (Supplementary Figure S2).

The third most abundant phylum was Cyanobacteria, that reached its maximal relative abundance (14.7 ± 5.7 % of the total community) in the 3-90 and 90-200 µm fractions microbiota, representative

of nano- and micro-phytoplankton (Figure 1C). The Cyanobacteria proportion decreased towards the small size-fraction microbiota (representing 6.0 ± 5.0 % of the community at 0.22 µm, 0.22-3 µm, and 0.22-90 µm) and towards the upper size fractions (representing 9.6 ± 4.5 % of the community in the > 200 µm fraction, representative of zooplankton) (Figure 3). Surprisingly, the absolute sequence number and relative proportion of Cyanobacteria were substantially higher in smaller volumes of filtered seawater (7.4 ± 3.5 % of the community for 2.5 L) than in larger volumes (3.4 ± 2.2 % of the prokaryotes for 4.5 L), when considering the 0.2-90 µm fraction obtained by sequential filtration. This could be explained by progressive clogging of the first 90 µm pre-filter by Cyanobacteria, due to their larger cell size, when larger volumes are filtered, thus reducing their representation on the subsequent 0.2 µm filter, while smaller prokaryotic cells can still pass through. Cyanobacteria were dominated by unaffiliated *Cyanobiaceae* and *Synechococcus* in all the size fractions (Figure 2; Supplementary Figure S3).

In the intermediate size fraction (3-90 µm), Proteobacteria and Bacteroidota taxa were still dominant, with relative abundances mostly similar to those in the lower size fractions. Some notable exceptions were SAR11 clade which decreased to half its value (8.2 ± 6.7 % of the community), while *Rhodobacteraceae* and *Flavobacteriaceae* slightly increased to 18.3 – 19.1 %, but were represented by different OTUs than in the other fractions (Supplementary Figure S2). Moreover, the Verrucomicrobiota phylum reached its highest proportion in the intermediate (3-90 µm) size fraction (10.9 ± 1.7% of the community), mostly represented by *Puniceicoccaceae* (*Lentimonas*).

In the largest size fractions (90-200 µm and > 200 µm), the relative abundances of Proteobacteria and Bacteroidota decreased (56.3 ± 11.3 % and 7.2 ± 4.9 % of the community, respectively), while other phyla emerged such as diverse Actinobacteriota (10.4 ± 5.3 %, mostly represented by *Cutibacterium* and *Microtrichaceae*) and Planctomycetota (7.6 ± 5.1 %, mostly represented by *Pirellulaceae*) (Figure 2, Supplementary Figure S2). Within Proteobacteria, new families emerged in large size fractions, such as *Oxalobacteraceae* (from Burkholderiales, all represented by the *Massilia* genus) and *Thioglobaceae* (from Pseudomonadales) both in the Gammaproteobacteria, and *Magnetospiraceae* (from Alphaproteobacteria), representing 2.0-7.0 % of the 90-200 µm fraction prokaryotes and 6.4-19.2 % of the > 200µm fraction, while they were not detected in the smaller size fractions (Figure 3, Supplementary Figure S2). Other taxa specifically enriched in the largest fraction (>200 µm) are *Acinetobacter* and *Spongiimonas* (Supplementary Figure S2).

Taxonomic determinants of the desorption pretreatment

After desorption pretreatment, Proteobacteria were highly predominant, representing 70 ± 18 % and 93 ± 7 % of the prokaryotes in the intermediate (3-90 µm) and large (90-200 and > 200 µm) size

fractions, respectively. This constitutes a drastic enrichment compared to the same size fractions without desorption. The major families of the intermediate size fraction after desorption were *Vibrionaceae* and *Rhodobacteraceae* (28.8 ± 11.6 % and 19.6 ± 5.8 % of the community, respectively), followed by *Alteromonadaceae* and *Pseudoalteromonadaceae* (10.2 ± 5.4 %), which strongly differed from the same size fraction without desorption (Figure 2). The genus *Glaciecola* was also discriminant of the 3-90 µm desorbed fraction (Figure 2). Most of the *Vibrionaceae* members in the 3-90 µm fraction were not affiliated at the genus level. Contrastingly, the largest size fractions (90-200 and > 200 µm) were dominated by *Vibrionaceae* (91.5 ± 7.4 % of the community), with distinct representative genera such as *Enterovibrio* (34 ± 21 % of the > 200 µm fraction only) or *Vibrio* (11.9 ± 0.7 % in both fractions) and *Photobacterium* (3.9 ± 1.8 % in both fractions) (Figure 2). *Vibrionaceae* were not or barely (< 0.1%) detected in the small (0.22 µm, 0.22-3 µm, 0.22-90 µm) and intermediate (3-90 µm) size fractions. In the large size fractions (90-200 µm and > 200 µm) without desorption pretreatment, *Vibrionaceae* represented no more than 0.8% of the community.

Variability of the post-extraction enrichment

The effect of prokaryotic DNA enrichment through Looxster treatment on the total community structure was low but significant (nested PERMANOVA with size fraction fixed as *strata* for permutations: $R^2 = 0.042$, p-value < 0.05). The effect of Looxster enrichment appears to be week on large size fractions (90-200 and > 200 µm), where, for all replicates, the closest relative of the treated sample was its untreated corresponding sample (Figure 1C). By contrast, in the small size fractions (0.22 µm, 0.22-3 µm, 0.22-90 µm) all the treated samples clustered together separated from their untreated corresponding samples, indicating a stronger effect of Looxster enrichment on community variation (Figure 1C).

However, the magnitude and direction of this effect was dependent on both the size fraction and the taxa considered. When considering the 12 most size-discriminating taxa (Figure 3), the Looxster treatment could lead to either over-abundance (e.g. *Rhodobacteraceae*, *Halieaceae*) or under-abundance (e.g. SAR11 clade, *Flavobacteriaceae*, *Thioglobaceae*) of some taxa within specific size fractions (Supplementary Table S4). Moreover, the Looxster treatment mainly affected the small size fractions for these concerned taxa.

DISCUSSION

Before the high-throughput sequencing era, the FL seawater community has been traditionally considered as more diverse than the PA one (Acinas et al., 1999; Ghiglione et al., 2009; Hollibaugh et

al., 2000; Kellogg & Deming, 2009). However, when using more resolutive approaches, an enhanced diversity is reported in PA (at different sizes) vs FL fractions (Bižić-Ionescu et al., 2015; Eloe et al., 2011; Rieck et al., 2015; Smith et al., 2013; Yeh & Fuhrman, 2022), similar to our findings, even though sampling depth can modulate this conclusion (Ganesh et al., 2014; Puigcorbé et al., 2023; Roth Rosenberg et al., 2021). Moreover, we showed an increased prokaryotic diversity with particle size, which has been previously interpreted as increasingly larger particles providing new microenvironmental niches (Mestre, Borrull, et al., 2017; Wei et al., 2020; Yeh & Fuhrman, 2022).

In the present work, the effect of the water volume filtered to obtain these different size fractions cannot be totally discarded. Even if we could not detect a significant effect of the different filtered volumes on the alpha-diversity, we observed a higher variability of Shannon index in large size fractions, which can be due to the higher seawater volume sampled for large size fractions, integrating a higher number of different particles, maybe heterogeneous across space, as previously observed (Yung et al., 2016). Data of 16S rRNA gene abundance could help resolving the effect of filtered volume. A previous study consistently showed that the volume of filtered water (ranging from 1 to 6 L) did not significantly affect the observed diversity, but induced variations in taxa abundances, without any apparent pattern in how abundances varied among volumes (Staley et al., 2015). Contrastingly, Padilla *et al.* (Padilla et al., 2015), reported that microbial community richness was more sensitive to the filtered water volume than to the filter pore size, and that richness followed opposing trends with increasing volume according to the considered size fraction. Overall, in comparison to these previous results, the effect of the filtered volume appears here to be negligible on community composition, as previously reported in the NW Mediterranean Sea (Ghiglione et al., 2009).

Here, we highlighted the variability of the prokaryotic assemblages along the planktonic size gradient. Several studies identified the size-fraction as the first parameter influencing the microbial community structure (Puigcorbé et al., 2023; Reintjes et al., 2023; Roth Rosenberg et al., 2021). By contrast, others pointed to different more important factors shaping the community structure, with different magnitude depending on the considered size-fraction, such as depth (especially impacting the small size fraction; (Mestre et al., 2018; Mestre, Ferrera, et al., 2017; Roth Rosenberg et al., 2021), or season (especially for large particles; (Mestre et al., 2020; Roth Rosenberg et al., 2021). The main taxa found in our study (Figure 3) are frequently reported as predominant in the Mediterranean Sea surface water (Coclet et al., 2019; Quéméneur et al., 2020; Zhou et al., 2018; Zouch et al., 2018) and in different temperate and tropical surface coastal seawaters (Baumas et al., 2021; Catão C. P. et al., 2021; Gilbert et al., 2012; Michotey et al., 2012; Smith et al., 2013). We identified SAR11 Clade I as discriminant for FL lifestyle, while *Flavobacteriaceae* and *Cyanobiaceae* were discriminant for PA lifestyle, which mirrors previous results (Catão C. P. et al., 2021; Ganesh et al., 2014; Mestre et al., 2020; Reintjes et al., 2023; Yung et al., 2016). The magnitude of dissimilarity between FL/PA communities is season-

dependent (Michotey et al., 2012; Rieck et al., 2015), which can be explained by the tight interaction and co-occurrence of some taxa (e.g. Bacteroidetes, Actinobacteria, Flavobacteraceae, and Verrucomicrobia) with phytoplankton blooms (Andersson et al., 2010; Nitin Parulekar et al., 2017; Rieck et al., 2015; Smith et al., 2013; Xu et al., 2021). In the present study, SAR11, *Flavobacteriaceae* and *Rhodobacteraceae* showed similar relative abundances at the time and place of sampling. However, at a larger scale, previous studies have reported opposite seasonal patterns for SAR11 and Rhodobacterales (Gilbert et al., 2012), and opposite geographic patterns for SAR11 and Flavobacteriia (Coclet et al., 2019). Mestre *et al.* (2020), showed different seasonal preference of SAR11 for different size fractions.

Several taxa enriched in the intermediate/large size fractions were also present in the smallest size fraction, as observed especially for *Rhodobacteraceae*, which suggests their potential role in aggregate formation. Indeed, *Rhodobacteraceae* are known as rapid and successful primary surface colonizers (Dang et al., 2008; Isaac et al., 2021), for instance in copepod microbiota (Gerdts et al., 2013) and phycosphere thanks to their tight adherence pilus gene (Isaac et al., 2021), and had been identified as key members of initial biofilm community in Eastern Mediterranean coastal seawater (Elifantz et al., 2013). The Flavobacteria class, abundant in PA-bacterioplankton, has been identified as primarily involved in the microbial colonization of diatom detritus (Abell & Bowman, 2005; Teeling et al., 2012) through different physiological features(Buchan et al., 2014), and potentially able to degrade alginate from macroalgae (Thomas et al., 2012). In previous studies, Planctomycetes (including *Pirellulaceae*), Bacteroidetes, Flavobacteriales and Verrucomicrobia (including Puniceicoccales) OTUs had been identified as discriminant of the larger size fractions in coastal seawater (Mestre et al., 2020; Mestre, Ferrera, et al., 2017; Reintjes et al., 2023; Yung et al., 2016), consistently with our results for the intermediate (Verrucomicrobia-enriched) and large (Planctomycetes-enriched) fractions. Through metagenome-assembled genomes (MAGs) reconstruction, Reintjes *et al.* (2023), showed that *Flavobacteriaceae*, *Planctomycetaceae*, *Puniceicoccaceae* and Verrucomicrobiales attached to small particles displayed key roles in the degradation of sulfated fucose-containing polysaccharides (i.e. the main constituent of the particles) through several enzymes such as glycoside hydrolase. Planctomycetes tend to a PA lifestyle and have been previously reported as associated with (micro)algae in the PA fraction, and involved in algal biomass mineralization (Kallscheuer et al., 2021; Rieck et al., 2015; Wiegand et al., 2021). Finally, two genera that are discriminant of the largest size fraction in our study (*Acinetobacter* and *Pseudomonas*) were also predominant in mesopelagic fast-sinking particles composed of phytodetrital aggregates and zooplankton fecal pellets (Baumas et al., 2021). Both genera are involved in organic matter degradation and have a potential specialization for attached lifestyle and biofilm formation. All together, these results show that the microbial variability

observed in our study can be consistently explained by the lifestyle of the different taxa and their preference for different niches along the planktonic size gradient.

The 0.22 µm filtration approach is commonly used to characterize the bulk prokaryotic diversity in aquatic ecosystems. Interestingly, here, we showed that the bulk community was most statistically similar to that of the 0.22-90 µm fraction for similar filtered volumes. The bulk approach is thus representative of the FL- and small size-fraction PA-microbiota, while it did not effectively capture the large size-fraction of PA-microbiota. This is further confirmed by the pairwise comparisons between the bulk and each size fraction, showing drastically different taxa in the large size-fractions while there were shared common taxa (with varying relative abundances) in the FL- and small size-fraction PA-microbiota (Supplementary Figure S2). In other words, the pre-filtration of seawater at 90 µm did not significantly modify the community structure compared to the bulk community. However, the pre-filtration provided a more reproducible and consistent picture of the prokaryotic communities among replicates, probably due to the removal of random big particles. Most studies on PA prokaryotes have used conventional bottle sampling coupled to size-fractionated filtration. However, this approach (i) can distort the community representation compared to in-situ filtering (Torres-Beltrán et al., 2019) and (ii) is considered to biasedly underestimate fast-sinking particles. The marine snow catcher method, developed to reduce particle-alteration during sampling, showed the same dichotomy as our results between fast-sinking (higher proportion of *Flavobacteriaceae*) and free-living (higher proportion of SAR11 Clade) communities (Baumas et al., 2021).

The effect of prokaryotic DNA enrichment through Looxster treatment is not predictable as we showed that it strongly varies according to the considered taxa and size fraction. This method has been previously reported to possibly infer a bias towards the under-representation of microorganisms with high level of CpG methylation (Shi et al., 2022), as well as modifications of bacterial abundances without consistent pattern according to the taxa (Glassing et al., 2015). Here, the fact that alpha diversity did not significantly changed after the treatment suggests that it did not improve the detection of prokaryotes, rather slightly altering some community members representation.

The desorption pretreatment of the intermediate and large size-fractions led to a strong enrichment in *Vibrionaceae* members. *Vibrionaceae* and (*Pseudo)alteromonadaceae* are among the most abundant members in the microbiota of marine copepods (Gerdts et al., 2013) and other zooplankton species (Preheim et al., 2011), leading to their enrichment in particles and large size fractions of seawater fractionation (Fontanez et al., 2015; Reintjes et al., 2023; Yung et al., 2016). Some *Vibrionaceae* species are mutualistic symbionts or pathogens of marine animals (Takemura et al., 2014) and are known to play an important role in the catabolism of chitin (Hirano et al., 2019; Hunt et al.,

2008). Even if they are usually rare in seawater, *Vibrio* species can bloom, representing temporarily up to >50% of the microbial community, in correlation with diatoms (Gilbert et al., 2012). *Pseudoalteromonadaceae* and *Vibrio* OTUs –including potential pathogens– have been identified as dominant microbiota members (up to 25% of the community) on pelagic *Sargassum* macroalgae (Michotey et al., 2020) and on marine plastic debris (De Tender et al., 2015; Kirstein et al., 2016; Zettler et al., 2013), but in all cases barely observed in surrounding seawater. The high abundance of *Vibrio* in *Sargassum* microbiota appeared to be related with high nutrient concentrations in surrounding water, high algal growth rate, and low zooplankton density (Michotey et al., 2020), which can explain the differences of *Vibrio* abundances with our results. In their study, Michotey *et al.* (2020) investigated the algal microbiota using a desorption protocol (agitation and sonication in a desorption buffer) similar to the one we evaluated in the present work, suggesting a possible misrepresentation of the prokaryotic community associated with *Sargassum* due to this pretreatment. First, desorption pretreatment might lead to the over-representation of easily detachable surface bacteria. Second, due to the general extremely fast growth rate of *Vibrio* genus representatives (Mouriño-Pérez et al., 2003; Weinstock et al., 2016), even at low temperature (Sheikh et al., 2022), and despite all the precautions taken here to apply the pretreatment as fast as possible, we cannot exclude that they grew during the desorption step (2 x 1h, 4°C), outcompeting other microbial community members. In Padilla *et al.*, the over-abundance of *Vibrio* (60% of the seawater community) was considered as a bias associated to low filtration volumes[29]. Overall, this result is a strong argument against the use of desorption as a pretreatment to recover plankton microbiota. For this reason, a direct DNA extraction approach (without cell desorption pretreatment nor prokaryotic DNA enrichment) was subsequently selected for the survey of prokaryotic diversity related to plankton along a North-South transect in the Mediterranean Sea in the frame of the MERITE-HIPPOCAMPE campaign (Tedetti et al., 2023). The objective of this subsequent survey will be (i) to assess the relations between prokaryotic diversity and organic/inorganic contaminants in an oceanographic basin strongly impacted by anthropogenic activities (Chifflet et al., 2023; Guigue et al., 2023; Tesán-Onrubia et al., 2023), and (ii) to determine the effect of prokaryotic composition on the accumulation, concentration and transfer of contaminants within the planktonic trophic web, i.e., bacterio-, phyto-, and zooplankton (Quéméneur et al., in preparation). It was therefore important to examine previously the effect of DNA extraction method from different plankton size fractions as proposed here.

Conclusion

In this study, we aimed to evaluate the methodological biases linked to plankton-microbiota characterization, by comparing different methodological approaches for DNA recovery, on different plankton size fractions. We showed that the first driver of microbial community differentiation was the plankton size fraction. The micro/mesozooplankton microbiota (> 90 µm) was characterized by the enrichment of *e.g.* Actinobacteriota, Planctomycetota, and some families of Gammaproteobacteria. The micro/nanophytoplankton (3-90µm) was characterized by the enrichment of *e.g.* Cyanobacteria, *Flavobacteriaceae*, and some Verrucomicrobiota. The free-living or small particle-attached microbiota (0.2-3 µm) was characterized by the enrichment of *e.g.* Alphaproteobacteria (SAR11 clade) and some Bacteroidota, while other taxa (e.g. *Rhodobacteraceae*) were abundant across low and intermediate fractions. Within the lowest size fraction, the generally used "bulk" approach (> 0.2 µm) was more representative of the 0.2-90 µm fraction, suggesting that the 90 µm pre-filtration does not modify the image of the community obtained by direct filtration. The prokaryotic DNA enrichment method (Looxster) altered taxa abundances without consistent pattern according to taxa and size fraction. The cell desorption pre-treatment induced a strong underestimation of the diversity and an over-representation of *Vibrionaceae*. Altogether, these results highlight the importance of a size-fractionated approach for plankton-microbiota studies, warning for a risk of clogging in case of high filtered volumes especially when using pre-filters. Therefore, we would recommend the direct extraction approach, without post-extraction enrichment, nor desorption step due to the resulting biased representation of the communities. These results might be dependent on the studied ecosystem, its trophic status, the water composition (nutrients, organic content, contaminants), and microbial community and planktonic assemblage compositions.

Author contributions

Léa Cabrol: Conceptualization; Methodology; Investigation; Formal analysis; Supervision; Writing - original draft

Mélanie Delleuze: Formal analysis; Visualization

Arthur Szylit: Data curation; Formal analysis; Visualization

Guillaume Schwob: Formal analysis; Visualization; Writing - review & editing

Marianne Quéméneur: Investigation; Methodology; Writing - review & editing

Benjamin Misson: Funding acquisition; Methodology; Investigation; Writing - review & editing

Funding, Acknowledgements

This work was supported by the MERITE-HIPPOCAMPE project, initiated and funded by the cross-disciplinary *Pollution & Contaminants* axis of the CNRS-INSU MISTRALS program (joint action of the MERMEX-MERITE and CHARMEX subprograms). The authors would like to thank Jean-Louis Jamet for his contribution to marine sampling and Emilie Paséro, Nicolas Gallois, and Ellouène Charavel for their contribution to molecular work. LC, MD, and GS would like to acknowledge funding from ANID Millennium Science Initiative Program ICN2021-002 (National research agency, Chile).

References

Abell, G. C. J., & Bowman, J. P. (2005). Ecological and biogeographic relationships of class Flavobacteria in the Southern Ocean. *FEMS Microbiology Ecology*, *51*(2), 265–277. https://doi.org/10.1016/j.femsec.2004.09.001

Acinas, S. G., Antón, J., & Rodríguez-Valera, F. (1999). Diversity of free-living and attached bacteria in offshore western Mediterranean waters as depicted by analysis of genes encoding 16S rRNA. *Applied and Environmental Microbiology*, *65*(2), 514–522. https://doi.org/10.1128/aem.65.2.514-522.1999

Aluru, N., Fields, D. M., Shema, S., Skiftesvik, A. B., & Browman, H. I. (2021). Gene expression and epigenetic responses of the marine Cladoceran, Evadne nordmanni, and the copepod, Acartia clausi, to elevated CO2. *Ecology and Evolution*, *11*(23), 16776–16785. https://doi.org/10.1002/ece3.8309

Andersson, A. F., Riemann, L., & Bertilsson, S. (2010). Pyrosequencing reveals contrasting seasonal dynamics of taxa within Baltic Sea bacterioplankton communities. *ISME Journal*, *4*(2), 171–181. https://doi.org/10.1038/ismej.2009.108

Baumas, C. M. J., Le Moigne, F. A. C., Garel, M., Bhairy, N., Guasco, S., Riou, V., Armougom, F., Grossart, H. P., & Tamburini, C. (2021). Mesopelagic microbial carbon production correlates with diversity across different marine particle fractions. *ISME Journal*, *15*(6), 1695–1708. https://doi.org/10.1038/s41396-020-00880-z

Bižić-Ionescu, M., Zeder, M., Ionescu, D., Orlić, S., Fuchs, B. M., Grossart, H. P., & Amann, R. (2015). Comparison of bacterial communities on limnic versus coastal marine particles reveals profound differences in colonization. *Environmental Microbiology*, *17*(10), 3500–3514. https://doi.org/10.1111/1462-2920.12466

Bogan, S. N., Johnson, K. M., & Hofmann, G. E. (2020). Changes in Genome-Wide Methylation and Gene Expression in Response to Future pCO2 Extremes in the Antarctic Pteropod Limacina helicina antarctica. *Frontiers in Marine Science*, *6*. https://doi.org/10.3389/fmars.2019.00788

Buchan, A., LeCleir, G. R., Gulvik, C. A., & González, J. M. (2014). Master recyclers: features and functions of bacteria associated with phytoplankton blooms. In *Nature reviews. Microbiology* (Vol. 12, Issue 10, pp. 686–698). https://doi.org/10.1038/nrmicro3326

Cabrol, L., Malhautier, L., Poly, F., Lepeuple, A. S., & Fanlo, J. L. (2010). Assessing the bias linked to DNA recovery from biofiltration woodchips for microbial community investigation by fingerprinting. *Applied Microbiology and Biotechnology*, *85*(3), 779–790. https://doi.org/10.1007/s00253-009-2253-8

Catão C. P., E., Pollet, T., Garnier, C., Barry-Martinet, R., Rehel, K., Linossier, I., Tunin-Ley, A., Turquet, J., & Briand, J. F. (2021). Temperate and tropical coastal waters share relatively similar microbial biofilm communities while free-living or particle-attached communities are distinct. *Molecular Ecology*, *30*(12), 2891–2904. https://doi.org/10.1111/mec.15929

Chifflet, S., Briant, N., Tesán-Onrubia, J. A., Zaaboub, N., Amri, S., Radakovitch, O., Bănaru, D., & Tedetti, M. (2023). Distribution and accumulation of metals and metalloids in planktonic food webs of the Mediterranean Sea (MERITE-HIPPOCAMPE campaign). *Marine Pollution Bulletin*, *186*. https://doi.org/10.1016/j.marpolbul.2022.114384

Chouvelon, T., Strady, E., Harmelin-Vivien, M., Radakovitch, O., Brach-Papa, C., Crochet, S., Knoery, J., Rozuel, E., Thomas, B., Tronczynski, J., & Chiffoleau, J. F. (2019). Patterns of trace metal bioaccumulation and trophic transfer in a phytoplankton-zooplankton-small pelagic fish marine food web. *Marine Pollution Bulletin*, *146*(February), 1013–1030. https://doi.org/10.1016/j.marpolbul.2019.07.047

Coclet, C., Garnier, C., Durrieu, G., Omanović, D., D'Onofrio, S., Le Poupon, C., Mullot, J. U., Briand, J. F., & Misson, B. (2019). Changes in bacterioplankton communities resulting from direct and indirect interactions with trace metal gradients in an urbanized marine coastal area. *Frontiers in Microbiology*, *10*(FEB). https://doi.org/10.3389/fmicb.2019.00257

D'Alelio, D., Eveillard, D., Coles, V. J., Caputi, L., Ribera d'Alcalà, M., & Iudicone, D. (2019). Modelling the complexity of plankton communities exploiting omics potential: From present challenges to an integrative pipeline. *Current Opinion in Systems Biology*, *13*, 68–74. https://doi.org/10.1016/j.coisb.2018.10.003

Dang, H., Li, T., Chen, M., & Huang, G. (2008). *Cross-Ocean Distribution of Rhodobacterales Bacteria as Primary Surface Colonizers in Temperate Coastal Marine Waters □ †*. *74*(1), 52–60. https://doi.org/10.1128/AEM.01400-07

De Mendoza, A., Bonnet, A., Vargas-Landin, D. B., Ji, N., Hong, F., Yang, F., Li, L., Hori, K., Pflueger, J., Buckberry, S., Ohta, H., Rosic, N., Lesage, P., Lin, S., & Lister, R. (2018). Recurrent acquisition of cytosine methyltransferases into eukaryotic retrotransposons. *Nature Communications*, *9*(1). https://doi.org/10.1038/s41467-018-03724-9

De Tender, C. A., Devriese, L. I., Haegeman, A., Maes, S., Ruttink, T., & Dawyndt, P. (2015). Bacterial Community Profiling of Plastic Litter in the Belgian Part of the North Sea. *Environmental Science and Technology*, *49*(16), 9629–9638. https://doi.org/10.1021/acs.est.5b01093

Elifantz, H., Horn, G., Ayon, M., Cohen, Y., & Minz, D. (2013). Rhodobacteraceae are the key members of the microbial community of the initial biofilm formed in Eastern Mediterranean coastal seawater. *FEMS Microbiology Ecology*, *85*(2), 348–357. https://doi.org/10.1111/1574-6941.12122

Eloe, E. A., Shulse, C. N., Fadrosh, D. W., Williamson, S. J., Allen, E. E., & Bartlett, D. H. (2011). Compositional differences in particle-associated and free-living microbial assemblages from an extreme deep-ocean environment. *Environmental Microbiology Reports*, *3*(4), 449–458. https://doi.org/10.1111/j.1758-2229.2010.00223.x

Fan, X., Han, W., Teng, L., Jiang, P., Zhang, X., Xu, D., Li, C., Pellegrini, M., Wu, C., Wang, Y., Kaczurowski, M. J. S., Lin, X., Tirichine, L., Mock, T., & Ye, N. (2020). Single-base methylome profiling of the giant kelp Saccharina japonica reveals significant differences in DNA methylation to microalgae and plants. *New Phytologist*, *225*(1), 234–249. https://doi.org/10.1111/nph.16125

Fontanez, K. M., Eppley, J. M., Samo, T. J., Karl, D. M., & DeLong, E. F. (2015). Microbial community structure and function on sinking particles in the North Pacific Subtropical Gyre. *Frontiers in Microbiology*, *6*(MAY). https://doi.org/10.3389/fmicb.2015.00469

Ganesh, S., Parris, D. J., Delong, E. F., & Stewart, F. J. (2014). Metagenomic analysis of size-fractionated picoplankton in a marine oxygen minimum zone. *ISME Journal*, *8*(1), 187–211. https://doi.org/10.1038/ismej.2013.144

Gerdts, G., Brandt, P., Kreisel, K., Boersma, M., Schoo, K. L., & Wichels, A. (2013). The microbiome of North Sea copepods. *Helgoland Marine Research*, *67*(4), 757–773. https://doi.org/10.1007/s10152-013-0361-4

Ghiglione, J. F., Conan, P., & Pujo-Pay, M. (2009). Diversity of total and active free-living vs. particle-attached bacteria in the euphotic zone of the NW Mediterranean Sea. *FEMS Microbiology Letters*, *299*(1), 9–21. https://doi.org/10.1111/j.1574-6968.2009.01694.x

Gilbert, J. A., Steele, J. A., Caporaso, J. G., Steinbrück, L., Reeder, J., Temperton, B., Huse, S., McHardy, A. C., Knight, R., Joint, I., Somerfield, P., Fuhrman, J. A., & Field, D. (2012). Defining seasonal marine microbial community dynamics. *ISME Journal*, *6*(2), 298–308. https://doi.org/10.1038/ismej.2011.107

Glassing, A., Dowd, S. E., Galandiuk, S., Davis, B., Jorden, J. R., & Chiodini, R. J. (2015). Changes in 16s RNA Gene Microbial Community Profiling by Concentration of Prokaryotic DNA. *Journal of Microbiological Methods*, *119*, 239–242. https://doi.org/10.1016/j.mimet.2015.11.001

Guigue, C., Tesán-Onrubia, J. A., Guyomarc'h, L., Bănaru, D., Carlotti, F., Pagano, M., Chifflet, S., Malengros, D., Chouba, L., Tronczynski, J., & Tedetti, M. (2023). Hydrocarbons in size-fractionated plankton of the Mediterranean Sea (MERITE-HIPPOCAMPE campaign). *Marine Pollution Bulletin*, *194*(Pt B), 115386. https://doi.org/10.1016/j.marpolbul.2023.115386

Göröcs, Z., Tamamitsu, M., Bianco, V., Wolf, P., Roy, S., Shindo, K., Yanny, K., Wu, Y., Koydemir, H. C., Rivenson, Y., & Ozcan, A. (2018). A deep learning-enabled portable imaging flow cytometer for cost-effective, high-throughput, and label-free analysis of natural water samples. *Light: Science and Applications*, *7*(1). https://doi.org/10.1038/s41377-018-0067-0

Hirano, T., Okubo, M., Tsuda, H., Yokoyama, M., Hakamata, W., & Nishio, T. (2019). Chitin Heterodisaccharide, Released from Chitin by Chitinase and Chitin Oligosaccharide Deacetylase, Enhances the Chitin- Metabolizing Ability of Vibrio parahaemolyticus. *Journal of Bacteriology*, *201*(20 e00270-19.), 1–13.

Hoguin, A., Yang, F., Groisillier, A., Bowler, C., Genovesio, A., Ait-Mohamed, O., Vieira, F. R. J., & Tirichine, L. (2023). The model diatom Phaeodactylum tricornutum provides insights into the

diversity and function of microeukaryotic DNA methyltransferases. *Communications Biology*, *6*(1). https://doi.org/10.1038/s42003-023-04629-0

Hollibaugh, J. T., Wong, P. S., & Murrell, M. C. (2000). Similarity of particle-associated and free-living bacterial communities in northern San Francisco Bay, California. *Aquatic Microbial Ecology*, *21*(2), 103–114. https://doi.org/10.3354/ame021103

Horner, R. A. (2002). *A Taxonomic Guide to Some Common Marine Phytoplankton* (Biopress Ltd, Ed.).

Hunt, D. E., Gevers, D., Vahora, N. M., & Polz, M. F. (2008). *Conservation of the Chitin Utilization Pathway in the Vibrionaceae □ †*. *74*(1), 44–51. https://doi.org/10.1128/AEM.01412-07

Isaac, A., Francis, B., Amann, R. I., & Amin, S. A. (2021). Tight Adherence (Tad) Pilus Genes Indicate Putative Niche Differentiation in Phytoplankton Bloom Associated Rhodobacterales. *Frontiers in Microbiology*, *12*. https://doi.org/10.3389/fmicb.2021.718297

Kallscheuer, N., Rast, P., Jogler, M., Wiegand, S., Kohn, T., Boedeker, C., Jeske, O., Heuer, A., Quast, C., Glöckner, F. O., Rohde, M., & Jogler, C. (2021). Analysis of bacterial communities in a municipal duck pond during a phytoplankton bloom and isolation of Anatilimnocola aggregata gen. nov., sp. nov., Lacipirellula limnantheis sp. nov. and Urbifossiella limnaea gen. nov., sp. nov. belonging to the phylum. *Environmental Microbiology*, *23*(3), 1379–1396. https://doi.org/10.1111/1462-2920.15341

Kellogg, C. T. E., & Deming, J. W. (2009). Comparison of free-living, suspended particle, and aggregate-associated bacterial and archaeal communities in the Laptev Sea. *Aquatic Microbial Ecology*, *57*(1), 1–18. https://doi.org/10.3354/ame01317

Kirstein, I. V., Kirmizi, S., Wichels, A., Garin-Fernandez, A., Erler, R., Löder, M., & Gerdts, G. (2016). Dangerous hitchhikers? Evidence for potentially pathogenic Vibrio spp. on microplastic particles. *Marine Environmental Research*, *120*, 1–8. https://doi.org/10.1016/j.marenvres.2016.07.004

Lavergne, C., Aguilar-Muñoz, P., Calle, N., Thalasso, F., Astorga-España, M. S., Sepulveda-Jauregui, A., Martinez-Cruz, K., Gandois, L., Mansilla, A., Chamy, R., Barret, M., & Cabrol, L. (2021). Temperature differently affected methanogenic pathways and microbial communities in sub-Antarctic freshwater ecosystems. *Environment International*, *154*. https://doi.org/10.1016/j.envint.2021.106575

Maugeri, T. L., Carbone, M., Fera, M. T., Irrera, G. P., & Gugliandolo, C. (2004). Distribution of potentially pathogenic bacteria as free living and plankton associated in a marine coastal zone. *Journal of Applied Microbiology*, *97*(2), 354–361. https://doi.org/10.1111/j.1365-2672.2004.02303.x

Mestre, M., Borrull, E., Sala, M., & Gasol, J. M. (2017). Patterns of bacterial diversity in the marine planktonic particulate matter continuum. *ISME Journal*, *11*(4), 999–1010. https://doi.org/10.1038/ismej.2016.166

Mestre, M., Ferrera, I., Borrull, E., Ortega-Retuerta, E., Mbedi, S., Grossart, H. P., Gasol, J. M., & Sala, M. M. (2017). Spatial variability of marine bacterial and archaeal communities along the particulate matter continuum. *Molecular Ecology*, *26*(24), 6827–6840. https://doi.org/10.1111/mec.14421

Mestre, M., Höfer, J., Sala, M. M., & Gasol, J. M. (2020). Seasonal Variation of Bacterial Diversity Along the Marine Particulate Matter Continuum. *Frontiers in Microbiology*, *11*. https://doi.org/10.3389/fmicb.2020.01590

Mestre, M., Ruiz-González, C., Logares, R., Duarte, C. M., Gasol, J. M., & Sala, M. M. (2018). Sinking particles promote vertical connectivity in the ocean microbiome. *Proceedings of the National Academy of Sciences of the United States of America*, *115*(29), E6799–E6807. https://doi.org/10.1073/pnas.1802470115

Michotey, V., Blanfuné, A., Chevalier, C., Garel, M., Diaz, F., Berline, L., Le Grand, L., Armougom, F., Guasco, S., Ruitton, S., Changeux, T., Belloni, B., Blanchot, J., Ménard, F., & Thibaut, T. (2020). In situ observations and modelling revealed environmental factors favouring occurrence of Vibrio in microbiome of the pelagic Sargassum responsible for strandings. *Science of the Total Environment*, *748*. https://doi.org/10.1016/j.scitotenv.2020.141216

Michotey, V., Guasco, S., Boeuf, D., Morezzi, N., Durieux, B., Charpy, L., & Bonin, P. (2012). Spatio-temporal diversity of free-living and particle-attached prokaryotes in the tropical lagoon of Ahe atoll (Tuamotu Archipelago) and its surrounding oceanic waters. *Marine Pollution Bulletin*, *65*(10–12), 525–537. https://doi.org/10.1016/j.marpolbul.2012.01.009

Mouriño-Pérez, R. R., Worden, A. Z., & Azam, F. (2003). Growth of Vibrio cholerae O1 in Red Tide Waters off California. *Applied and Environmental Microbiology*, *69*(11), 6923–6931. https://doi.org/10.1128/AEM.69.11.6923-6931.2003

Nitin Parulekar, N., Kolekar, P., Jenkins, A., Kleiven, S., Utkilen, H., Johansen, A., Sawant, S., Kulkarni-Kale, U., Kale, M., & Sæbø, M. (2017). Characterization of bacterial community associated with phytoplankton bloom in a eutrophic lake in South Norway using 16S rRNA gene amplicon sequence analysis. *PLoS ONE*, *12*(3), 1–22. https://doi.org/10.1371/journal.pone.0173408

Padilla, C. C., Ganesh, S., Gantt, S., Huhman, A., Parris, D. J., Sarode, N., & Stewart, F. J. (2015). Standard filtration practices may significantly distort planktonic microbial diversity estimates. *Frontiers in Microbiology*, *6*(JUN), 1–10. https://doi.org/10.3389/fmicb.2015.00547

Pouch, A., Zaborska, A., Dąbrowska, A. M., & Pazdro, K. (2022). Bioaccumulation of PCBs, HCB and PAHs in the summer plankton from West Spitsbergen fjords. *Marine Pollution Bulletin*, *177*(March). https://doi.org/10.1016/j.marpolbul.2022.113488

Preheim, S. P., Boucher, Y., Wildschutte, H., David, L. A., Veneziano, D., Alm, E. J., & Polz, M. F. (2011). *Metapopulation structure of Vibrionaceae among*. *13*, 265–275. https://doi.org/10.1111/j.1462-2920.2010.02328.x

Puigcorbé, V., Ruiz-González, C., Masqué, P., & Gasol, J. M. (2023). Impact of particle flux on the vertical distribution and diversity of size-fractionated prokaryotic communities in two East Antarctic polynyas. *Frontiers in Microbiology*, *14*. https://doi.org/10.3389/fmicb.2023.1078469

Quéméneur, M., Bel Hassen, M., Armougom, F., Khammeri, Y., Lajnef, R., & Bellaaj-Zouari, A. (2020). Prokaryotic Diversity and Distribution Along Physical and Nutrient Gradients in the Tunisian Coastal Waters (South Mediterranean Sea). *Frontiers in Microbiology*, *11*(December), 1–14. https://doi.org/10.3389/fmicb.2020.593540

Reintjes, G., Heins, A., Wang, C., & Amann, R. (2023). Abundance and composition of particles and their attached microbiomes along an Atlantic Meridional Transect. *Frontiers in Marine Science*, *10*. https://doi.org/10.3389/fmars.2023.1051510

Rieck, A., Herlemann, D. P. R., Jürgens, K., & Grossart, H. P. (2015). Particle-associated differ from free-living bacteria in surface waters of the baltic sea. *Frontiers in Microbiology*, *6*(DEC). https://doi.org/10.3389/fmicb.2015.01297

Rodrigues, S. M., Elliott, M., Almeida, C. M. R., & Ramos, S. (2021). Microplastics and plankton: Knowledge from laboratory and field studies to distinguish contamination from pollution. *Journal of Hazardous Materials*, *417*(May), 126057. https://doi.org/10.1016/j.jhazmat.2021.126057

Roth Rosenberg, D., Haber, M., Goldford, J., Lalzar, M., Aharonovich, D., Al-Ashhab, A., Lehahn, Y., Segrè, D., Steindler, L., & Sher, D. (2021). Particle-associated and free-living bacterial communities in an oligotrophic sea are affected by different environmental factors. *Environmental Microbiology*, *23*(8), 4295–4308. https://doi.org/10.1111/1462-2920.15611

Rubiola, S., Chiesa, F., Dalmasso, A., Di Ciccio, P., & Civera, T. (2020). Detection of Antimicrobial Resistance Genes in the Milk Production Environment: Impact of Host DNA and Sequencing Depth. *Frontiers in Microbiology*, *11*(August). https://doi.org/10.3389/fmicb.2020.01983

Sheikh, H. I., Najiah, M., Fadhlina, A., Laith, A. A., Nor, M. M., Jalal, K. C. A., & Kasan, N. A. (2022). Temperature Upshift Mostly but not Always Enhances the Growth of Vibrio Species: A Systematic Review. In *Frontiers in Marine Science* (Vol. 9). Frontiers Media S.A. https://doi.org/10.3389/fmars.2022.959830

Shi, Y., Wang, G., Lau, H. C. H., & Yu, J. (2022). Metagenomic Sequencing for Microbial DNA in Human Samples: Emerging Technological Advances. *International Journal of Molecular Sciences*, *23*(4). https://doi.org/10.3390/ijms23042181

Sieburth, John McN; Jürgen Lenz, V. S. (1978). Pelagic ecosystem structure: Heterotrophic compartments of the plankton and their relationship to plankton size fractions. *Limnology and Oceanography*, *23*(6), 1256–1263. https://doi.org/10.4319/lo.1978.23.6.1256

Siokou-Frangou, I., Christaki, U., Mazzocchi, M. G., Montresor, M., Ribera D'Alcala, M., Vaque, D., & Zingone, A. (2010). Plankton in the open mediterranean Sea: A review. *Biogeosciences*, *7*(5), 1543–1586. https://doi.org/10.5194/bg-7-1543-2010

Smith, M. W., Allen, L. Z., Allen, A. E., Herfort, L., & Simon, H. M. (2013). Contrasting genomic properties of free-living and particle-attached microbial assemblages within a coastal ecosystem. *Frontiers in Microbiology*, *4*(MAY), 1–20. https://doi.org/10.3389/fmicb.2013.00120

Staley, C., Gould, T. J., Wang, P., Phillips, J., Cotner, J. B., & Sadowsky, M. J. (2015). Evaluation of water sampling methodologies for amplicon-based characterization of bacterial community structure. *Journal of Microbiological Methods*, *114*, 43–50. https://doi.org/10.1016/j.mimet.2015.05.003

Takemura, A. F., Chien, D. M., & Polz, M. F. (2014). Associations and dynamics of vibrionaceae in the environment, from the genus to the population level. *Frontiers in Microbiology*, *5*(FEB), 1–26. https://doi.org/10.3389/fmicb.2014.00038

Tedetti, M., Tronczynski, J., Carlotti, F., Pagano, M., Ismail, S. Ben, Sammari, C., Hassen, M. B., Desboeufs, K., Poindron, C., Chifflet, S., Zouari, A. B., Abdennadher, M., Amri, S., Bănaru, D., Abdallah, L. Ben, Bhairy, N., Boudriga, I., Bourin, A., Brach-Papa, C., … Garnier, C. (2023). Contamination of planktonic food webs in the Mediterranean Sea: Setting the frame for the

MERITE-HIPPOCAMPE oceanographic cruise (spring 2019). *Marine Pollution Bulletin*, *189*. https://doi.org/10.1016/j.marpolbul.2023.114765

Teeling, H., Fuchs, B. M., Becher, D., Klockow, C., Gardebrecht, A., Bennke, C. M., Kassabgy, M., Huang, S., Mann, A. J., Waldmann, J., Weber, M., Klindworth, A., Otto, A., Lange, J., Bernhardt, J., Reinsch, C., Hecker, M., Peplies, J., Bockelmann, F. D., … Amann, R. (2012). Substrate-controlled succession of marine bacterioplankton populations induced by a phytoplankton bloom. *Science*, *336*(6081), 608–611. https://doi.org/10.1126/science.1218344

Tesán-Onrubia, J. A., Heimbürger-Boavida, L. E., Dufour, A., Harmelin-Vivien, M., García-Arévalo, I., Knoery, J., Thomas, B., Carlotti, F., Tedetti, M., & Bănaru, D. (2023). Bioconcentration, bioaccumulation and biomagnification of mercury in plankton of the Mediterranean Sea. *Marine Pollution Bulletin*, *194*. https://doi.org/10.1016/j.marpolbul.2023.115439

Thomas, F., Barbeyron, T., Tonon, T., Génicot, S., Czjzek, M., & Michel, G. (2012). *Characterization of the first alginolytic operons in a marine bacterium : from their emergence in marine Flavobacteriia to their independent transfers to marine Proteobacteria and human gut Bacteroides*. *14*, 2379–2394. https://doi.org/10.1111/j.1462-2920.2012.02751.x

Tirichine, L., Rastogi, A., & Bowler, C. (2017). Recent progress in diatom genomics and epigenomics. *Current Opinion in Plant Biology*, *36*, 46–55. https://doi.org/10.1016/j.pbi.2017.02.001

Torres-Beltrán, M., Mueller, A., Scofield, M., Pachiadaki, M. G., Taylor, C., Tyshchenko, K., Michiels, C., Lam, P., Ulloa, O., Jürgens, K., Hyun, J. H., Edgcomb, V. P., Crowe, S. A., & Hallam, S. J. (2019). Sampling and processing methods impact microbial community structure and potential activity in a seasonally anoxic fjord: Saanich inlet, British Columbia. *Frontiers in Marine Science*, *6*(MAR). https://doi.org/10.3389/fmars.2019.00132

Traller, J. C., Cokus, S. J., Lopez, D. A., Gaidarenko, O., Smith, S. R., McCrow, J. P., Gallaher, S. D., Podell, S., Thompson, M., Cook, O., Morselli, M., Jaroszewicz, A., Allen, E. E., Allen, A. E., Merchant, S. S., Pellegrini, M., & Hildebrand, M. (2016). Genome and methylome of the oleaginous diatom Cyclotella cryptica reveal genetic flexibility toward a high lipid phenotype. *Biotechnology for Biofuels*, *9*(1). https://doi.org/10.1186/s13068-016-0670-3

Veluchamy, A., Lin, X., Maumus, F., Rivarola, M., Bhavsar, J., Creasy, T., O'Brien, K., Sengamalay, N. A., Tallon, L. J., Smith, A. D., Rayko, E., Ahmed, I., Crom, S. Le, Farrant, G. K., Sgro, J. Y., Olson, S. A., Bondurant, S. S., Allen, A., Rabinowicz, P. D., … Tirichine, L. (2013). Insights into the role of DNA methylation in diatoms by genome-wide profiling in Phaeodactylum tricornutum. *Nature Communications*, *4*. https://doi.org/10.1038/ncomms3091

Wagner Mackenzie, B., Waite, D. W., Biswas, K., Douglas, R. G., & Taylor, M. W. (2018). Assessment of microbial DNA enrichment techniques from sino-nasal swab samples for metagenomics. *Rhinology Online*, *1*(1), 160–193. https://doi.org/10.4193/rhinol/18.052

Wang, Y., & Qian, P. Y. (2009). Conservative fragments in bacterial 16S rRNA genes and primer design for 16S ribosomal DNA amplicons in metagenomic studies. *PLoS ONE*, *4*(10). https://doi.org/10.1371/journal.pone.0007401

Wei, G., Shan, D., Li, G., Li, X., Tian, R., He, J., & Shao, Z. (2020). Prokaryotic communities vary with floc size in a biofloc-technology based aquaculture system. *Aquaculture*, *529*. https://doi.org/10.1016/j.aquaculture.2020.735632

828 Weinstock, M. T., Hesek, E. D., Wilson, C. M., & Gibson, D. G. (2016). Vibrio natriegens as a fast-
829 growing host for molecular biology. *Nature Methods*, *13*(10), 849–851.
830 https://doi.org/10.1038/nmeth.3970

831 Wiegand, S., Rast, P., Kallscheuer, N., Jogler, M., Heuer, A., Boedeker, C., Jeske, O., Kohn, T.,
832 Vollmers, J., Kaster, A. K., Quast, C., Glöckner, F. O., Rohde, M., & Jogler, C. (2021). Analysis of
833 bacterial communities on north sea macroalgae and characterization of the isolated
834 planctomycetes adhaeretor mobilis gen. Nov., sp. nov., roseimaritima multifibrata sp. nov.,
835 rosistilla ulvae sp. nov. and rubripirellula lacrimiformis sp. nov. *Microorganisms*, *9*(7), 1–33.
836 https://doi.org/10.3390/microorganisms9071494

837 Wiesinger-Mayr, H., Jordana-Lluch, E., Martró, E., Schoenthaler, S., & Noehammer, C. (2011).
838 Establishment of a semi-automated pathogen DNA isolation from whole blood and comparison
839 with commercially available kits. *Journal of Microbiological Methods*, *85*(3), 206–213.
840 https://doi.org/10.1016/j.mimet.2011.03.003

841 Xu, S., He, C., Song, S., & Li, C. (2021). Spatiotemporal dynamics of marine microbial communities
842 following a Phaeocystis bloom: biogeography and co-occurrence patterns. *Environmental*
843 *Microbiology Reports*, *13*(3), 294–308. https://doi.org/10.1111/1758-2229.12929

844 Yeh, Y.-C., & Fuhrman, J. A. (2022). Contrasting diversity patterns of prokaryotes and protists over
845 time and depth at the San-Pedro Ocean Time series. *ISME Communications*, *2*(1), 1–12.
846 https://doi.org/10.1038/s43705-022-00121-8

847 Yung, C. M., Ward, C. S., Davis, K. M., Johnson, Z. I., & Hunt, D. E. (2016). Insensitivity of diverse and
848 temporally variable particle-associated microbial communities to bulk seawater environmental
849 parameters. *Applied and Environmental Microbiology*, *82*(11), 3431–3437.
850 https://doi.org/10.1128/AEM.00395-16

851 Zettler, E. R., Mincer, T. J., & Amaral-Zettler, L. A. (2013). Life in the 'plastisphere': Microbial
852 communities on plastic marine debris. *Environmental Science and Technology*, *47*(13), 7137–
853 7146. https://doi.org/10.1021/es401288x

854 Zhou, J., Song, X., Zhang, C. Y., Chen, G. F., Lao, Y. M., Jin, H., & Cai, Z. H. (2018). Distribution Patterns
855 of Microbial Community Structure Along a 7000-Mile Latitudinal Transect from the
856 Mediterranean Sea Across the Atlantic Ocean to the Brazilian Coastal Sea. *Microbial Ecology*,
857 *76*(3), 592–609. https://doi.org/10.1007/s00248-018-1150-z

858 Zouch, H., Cabrol, L., Chifflet, S., Tedetti, M., Karray, F., Zaghden, H., Sayadi, S., & Quéméneur, M.
859 (2018). Effect of Acidic Industrial Effluent Release on Microbial Diversity and Trace Metal
860 Dynamics During Resuspension of Coastal Sediment. *Frontiers in Microbiology*, *9*(December).
861 https://doi.org/10.3389/fmicb.2018.03103

862

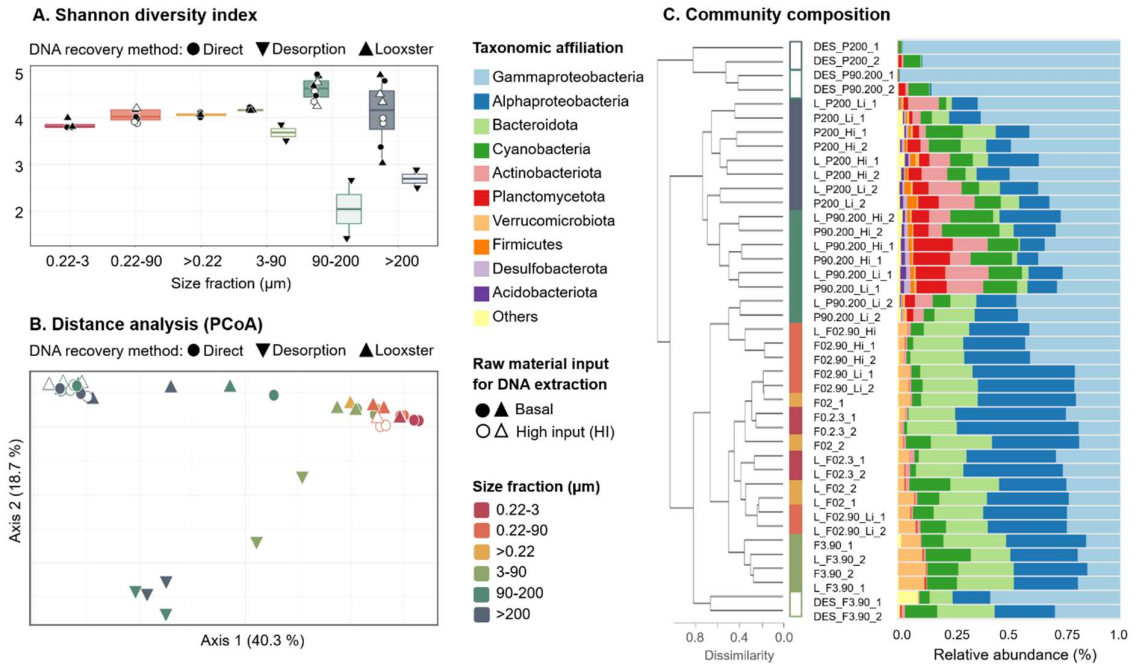

Figure 1. Representation of plankton-associated microbiome. A. Boxplot of the Shannon diversity index according to the planktonic size fraction and the DNA recovery method. Full symbols represent samples obtained from basal amount of raw material (water volume or plankton weight), while empty symbols represent samples obtained from higher amount of raw material. **B.** Ordination of microbial community variation by Principal Coordinate Analysis (PCoA) based on Bray Curtis dissimilarity index computed from the whole OTU abundance table. Samples are colored according to the planktonic size fraction. Symbol shapes indicate the DNA recovery methodology. Full and empty symbols represent samples obtained from, respectively, basal and high amount of raw material (water volume or plankton weight). The percentage of explained variance is indicated next to each axis. **C.** Barplot of microbial community composition at the phylum level, showing the relative abundance of the 9 most abundant phyla (dividing the Proteobacteria phylum into its two main classes), representing 98.9 ± 1.5 % of the community on average. The "Others" group encompasses phyla representing less than 0.2 % of the community each (0.9 % in total) and unaffiliated sequences (0.2 % in total). The samples are ordered according to Bray Curtis dissimilarity-based clustering. The resulting dendrogram (average linkage method) is shown on the left of the barplot. The sample names follow the nomenclature presented in Table 1 (*'DES'*: desorption pre-treatment; *'L'*: Looxster enrichment; *'Hi'*: high input; *'Li'*: low input; *'F'*: filters from water bottles; *'P'*: raw plankton from nets). The last digit corresponds to the biological replicate. The color code along the sample names indicates the corresponding planktonic size fraction.

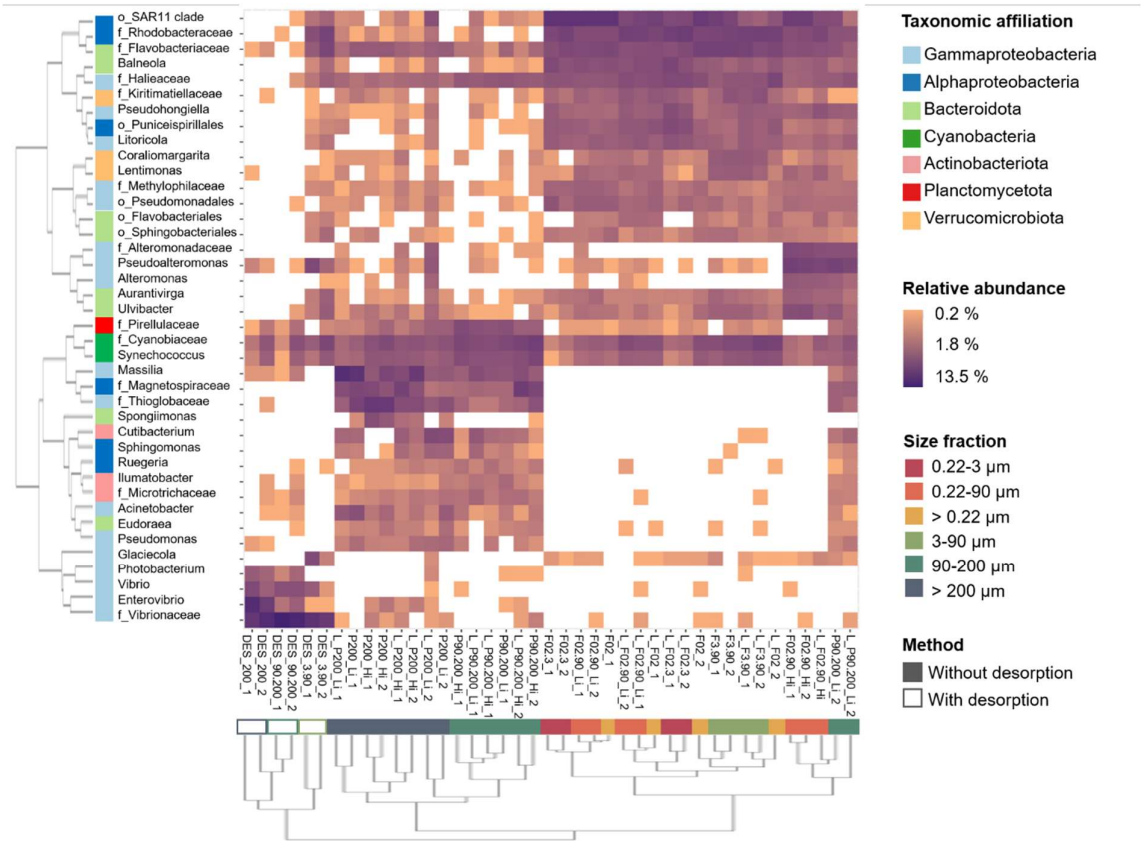

Figure 2. Representation of discriminant microbial taxa. Discriminant OTUs were previously identified by LDA (see Material and Methods) for each planktonic size fraction and DNA recovery methodology. The resulting 72 OTUs were aggregated at the genus level (or at the last available taxonomic rank when genus affiliation is not available) and filtered on abundance (> 0.1 %), resulting in 40 taxa. The heatmap shows the (log-transformed) relative abundance of these 40 taxa. The samples are ordered according to a clustering based on Bray-Curtis dissimilarity index computed from the abundance of these 39 taxa. The resulting dendrogram is shown at the bottom (average linkage method). The sample names follow the nomenclature presented in Table 1 (*'DES'*: desorption pre-treatment; *'L'*: Looxster enrichment; *'Hi'*: high input; *'Li'*: low input). The last digit corresponds to the biological replicate. The color code along the sample names indicates the corresponding planktonic size fraction. The taxa are ordered according to Bray-Curtis dissimilarity-based clustering (Ward.D2 linkage method). The color code along the taxa names indicates the corresponding taxonomic affiliation at the phylum level (following the same nomenclature as in Figure 1). The first digit in the taxa names indicates the higher available taxonomic rank when genus affiliation is not available.

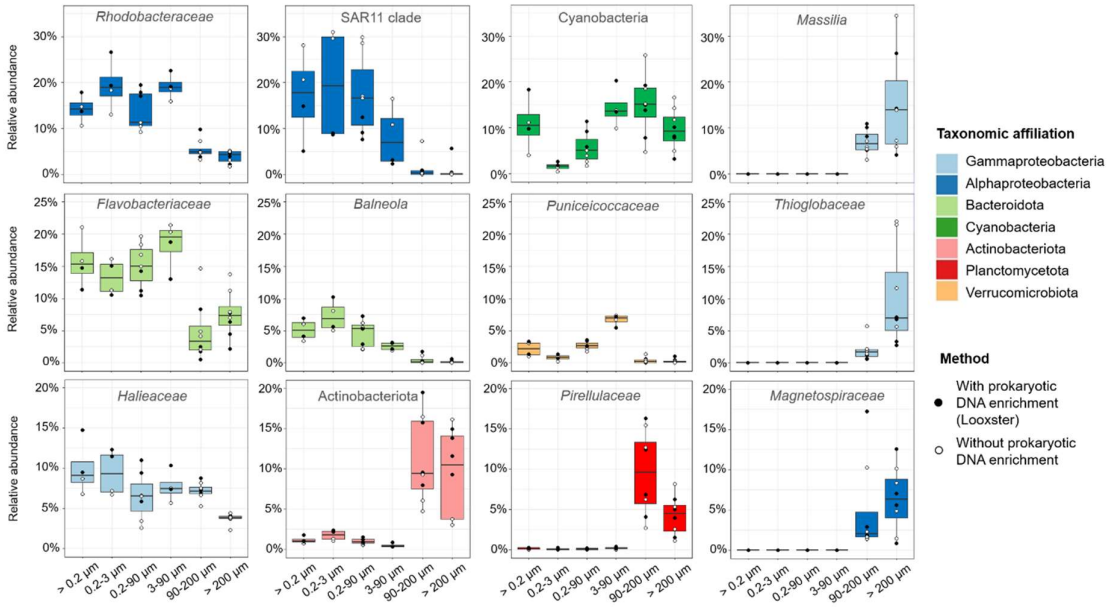

Figure 3. Boxplots representing the abundances of the most discriminant taxa along the plankton size fraction gradient. The median, first and third quartiles were calculated using all conditions excluding the desorption pre-treatment. White dots represent direct extraction, black dots represent post-treatment conditions (Looxster enrichment of prokaryotic DNA). Taxa are colored by phylum (or class for Proteobacteria). The selection of the most discriminant taxa is based on LDA analysis, as visualized on Figure 2.

SUPPLEMENTARY MATERIAL FOR:

Assessing the diversity of plankton-associated microbiota: a methodological evaluation

Authors :

Léa Cabrol[a,b,c], Mélanie Delleuze[b,d], Arthur Szylit[c], Guillaume Schwob[b,d,e], Marianne Quéméneur[a], Benjamin Misson[f]

CONTENTS:

Material and Methods | Desorption buffer composition

The raw plankton matrix was resuspended at a 1:5 w/v ratio in a sterile solution containing a desorption buffer (88% v/v), Tween80 detergent (0.06 % v/v) and 10 mM sodium pyrophosphate (12% v/v). The desorption buffer contained NaCl (26.3 g L^{-1}), KCl (0.745 g L^{-1}), Na_2SO_4 (0.99 g L^{-1}), $NaHCO_3$ (0.04 g L^{-1}) and EDTA (2.92 g L^{-1}), as adapted from Burke *et al.* 2009.

Material and Methods | DNA extraction protocol.

Preparation of 200 mL of buffer and lysis solutions (Tris and EDTA solutions are prepared separately):

- EDTA 0.5 M (pH = 8.0)
- Tris 1 M (pH = 8.0)
- NaCl 0.5 M
- sodium acetate 3 M

1. Preparation of 20 mL lysis buffer: final concentrations: Tris 20 mM, EDTA 25 mM, NaCl 50 mM, qsp ultrapure water. The solution is filter-sterilized and thoroughly mixed.

2. In each 15 mL falcon tube, before adding the samples, insert lysing beads (e.g. lysing matrix E, MPBio, containing 1.4 mm ceramic spheres, 0.1 mm silica spheres and one 4 mm glass bead). Add the sample (filter or solid). Add 2 mL of lysis buffer, vortex for 5 min, and cool on ice for 10 min.

3. Add 40 µL of lysozyme (from the stock solution at 50 mg/mL stored at -20°C) per tube (giving a final concentration of 1 mg/mL), vortex, and incubate at 37°C for 15 min.

4. Add 10% v/v (i.e. 200 µL) of SDS (stock 10 %) per tube, vortex.

5. Add 10 µL proteinase K (Qiagen, 600 mAU/ml solution, i.e. 20 mg/mL, or 40 mAU/mg protein), incubate at 56°C for 30 min.

6. Under extractor hood, add volume/volume of phenol:chloroform:isoamyl alcohol 25:24:1 (PCI1) (Sigma P2069, saturated with 10 mM Tris, pH 8, 1 mM EDTA) using only the lower phase of PCI. Shake by hand for 1.5 min.

7. Centrifuge at 4500 rpm for 20 min, and collect the supernatant in a new 15 mL falcon tube, by pipetting without touching the interface.

8. Add again volume/volume of phenol-chloroform-isoamyl alcohol 25:24:1 saturated with 10 mM Tris, pH 8, 1 mM EDTA (PCI2) using only the lower phase of PCI. Shake by hand for 1.5 min.

9. Centrifuge at 4500 rpm for 20 min, and collect the supernatant in a new 15 mL falcon tube, by pipetting without touching the interface.

10. Add volume/volume of Chloroform:Isoamyl alcohol 48:2, and shake by hand for 1.5 min.

11. Centrifuge at 4500 rpm for 20 min, and collect the supernatant in a new 15 mL falcon tube, by pipetting without touching the interface.

12. Precipitate the DNA in 0.6 volume of isopropanol, and add 10 % (of the total obtained volume) of sodium acetate (3 M, pH 6.0). Shake slowly by inversion for 1.5 min for DNA precipitation, and wait for 5 min at ambient temperature.

13. Centrifuge half of the obtained solution at 14000g for 20 minutes in a 2 mL Eppendorf tube. Discard the supernatant and add the other half volume in the same Eppendorf tube. Centrifuge at 14000g for 20 minutes.

14. Add 500 µL frozen ethanol 70% and resuspend the visible DNA pellets.

15. Centrifuge for 10 min at 14000 g and discard supernatant. Dry the tubes open on paper. Centrifuge the open empty tubes for 14000 g at 5 min. Dry the tubes open upside down on paper for 1 h.

16. Add 50 µL of ultrapure nuclease-free water and 1 µL of RNase (Sigma, solution 50% glycerol 10 mM Tris-HCl pH 8), resuspend the pellet for 30 min, vortex at very low speed.

17. Store at -20°C.

Material and Methods | Bioinformatic analysis.

The dataset of 2,185,748 initial raw sequences was processed with the FROGS pipeline (V 3.2.3) on the Galaxy platform (Escudie et al., 2018). Forward and reverse reads were merged with *Vsearch* authorizing 10% mismatch rate on the overlap region (minimal 10 bp overlap authorized, approximately 85 bp in our case). Preprocess included the recovery of correct sequences for both primers with *cutadapt* (accepting for 10% of differences in the primer sequences), size filtration (300-600 bp), and removal of ambiguous nucleotides (N), resulting in 65.7 % of clean sequences. The sequences were clustered into OTUs through the Swarm algorithm with fastidious option, using an aggregation distance clustering d=1 (Mahé et al. 2015), which does not impose arbitrary dissimilarity threshold for OTU definition. The chimeric sequences were then removed using *vsearch*, resulting in 1,001,366 kept sequences, grouped in 121,695 OTUs. Sequences present in less than 2 samples and with an abundance lower than 0.005% of the total sequence number (as recommended by Bokulich et al., 2013) were filtered out, resulting in a final number of 813 230 sequences clustered in 971 OTUs. We obtained, on average, 439 ± 88 OTUs per sample, with 19 835 ± 9 831 sequences per sample. The numbers of sequences and OTUs after each treatment step are provided in Supplementary Table S2 for each sample type.

Supplementary Table S1 | Filtered volumes of seawater for each size class. The colored lanes indicate the conditions for which different input volumes were tested.

Sample	Filtered volume (L)
F02-1	2.5
F02-2	2.5
F02.3-1	5
F02.3-2	5
F02.90-Li-1	2.5
F02.90-Li-2	2.5
F02.90-Hi-1	4
F02.90-Hi-2	4
F3.90-1	2.5
F3.90-2	2.5
DES-F3.90-1	5
DES-F3.90-2	5
P90.200-Li-1	490
P90.200-Li-2	490
P90.200-Hi-1	1959
P90.200-Hi-2	1959
DES-P90.200-1	4897
DES-P90.200-2	4897
P200-Li-1	1553
P200-Li-2	1553
P200-Hi-1	6213
P200-Hi-2	6213
DES-P200-1	21746
DES-P200-2	21746

Supplementary Table S2 | Results of the different steps of sequencing treatment process. The replicate values have been averaged.

			Number of sequences at the different stages of Pre-process					% of		Chimera removal		Filtration (abundance > 0.005%, prevalence > 2	
	Sample name	Raw reads before process	paired-end assembled	with 5' primer	with 3' primer	with expected length	without N	sequences kept after preprocess	Number of OTUs	Number of OTUs without chimera	Number of sequences without chimera	Number of OTUs after filtration	Number of sequences after filtration
Desorption	DES_3.90	69 060	66 138	54 291	54 111	54 086	54 067	78	13 631	4 509	37 196	423	32 259
	DES_90.200	56 124	47 818	38 929	38 806	38 757	38 747	69	6 645	4 296	35 793	338	31 197
	DES_200	62 396	53 240	41 417	41 269	41 195	41 177	66	7 528	4 624	35 674	341	30 227
Filtering size fractionnation	F02	61 386	58 435	49 423	49 278	49 262	49 235	80	16 141	4 829	32 068	468	27 025
	F0.2.3	50 612	48 354	40 525	40 389	40 378	40 363	80	11 713	3 308	26 038	343	22 714
	F02.90_Li	58 067	55 504	41 127	40 984	40 973	40 958	73	13 899	4 232	27 069	473	22 780
	F02.90_Hi	60 738	58 092	47 741	47 579	47 566	47 546	78	15 011	4 071	30 033	435	25 923
	F3.90	57 075	54 274	45 789	45 655	45 634	45 618	80	15 291	4 807	30 119	501	25 209
Filtering size fractionnation + Looxster enrichment	L_F02	62 289	59 351	46 567	46 399	46 371	46 351	75	13 842	4 604	31 595	499	27 002
	L_F02.3	58 640	55 889	47 659	47 490	47 471	47 448	81	13 318	3 727	29 399	352	25 600
	L_F02.90_Li	47 155	44 900	38 494	38 373	38 355	38 339	81	13 136	3 969	24 479	510	20 673
	L_F02.90_Hi	55 422	52 905	45 747	45 590	45 569	45 540	82	15 732	4 033	27 397	454	23 383
	L_F3.90	61 966	59 203	49 258	49 107	49 083	49 055	79	14 980	5 035	33 583	545	28 544
Plankton nets	P90.200_Li	45 523	33 259	26 560	26 447	26 183	26 167	58	10 765	4 780	19 649	569	13 633
	P90.200_Hi	49 050	32 330	22 907	22 845	22 747	22 739	44	11 153	5 179	16 395	482	10 009
	P200_Li	49 834	33 245	24 293	24 123	12 604	12 594	23	4 864	2 104	9 691	345	6 645
	P200_Hi	36 086	18 982	9 952	9 914	9 712	9 704	26	4 767	2 474	7 221	388	4 748
Plankton nets + Looxster enrichment	L_P90.200_Li	44 608	35 437	27 705	27 547	27 050	27 040	60	11 997	4 254	18 830	515	12 408
	L_P90.200_Hi	44 249	30 679	24 362	24 284	24 122	24 110	50	11 454	4 644	16 927	443	10 429
	L_P200_Li	49 180	37 149	26 888	26 803	24 774	24 764	44	9 355	3 227	18 177	412	13 392
	L_P200_Hi	41 130	18 434	9 166	9 127	8 984	8 979	23	4 056	2 235	7 053	395	4 510
Total sum all samples		2 185 748			1 466 640	1 436 169	1 435 531		359 020	123 695	1 001 366	971	813 230
Average per sample (SD)							35 013 (15 752)		11 288 (4838)	4045 (1350)	24 424 (10 690)	439 (88)	19 835 (9 831)

Supplementary Table S3 | Values of alpha diversity

		Mean Shannon diversity index	Standard deviation
Desorption	DES_3.90	3.68	0.24
	DES_90.200	2.05	0.88
	DES_200	2.70	0.27
Filtering size fractionnation	F02	4.06	0.08
	F0.2.3	3.80	0.00
	F02.90_Li	4.00	0.02
	F02.90_Hi	3.89	0.02
	F3.90	4.19	0.05
Filtering size fractionnation + Looxster enrichment	L_F02	4.06	0.01
	L_F02.3	3.90	0.13
	L_F02.90_Li	4.17	0.00
	L_F02.90_Hi	4.20	na
	L_F3.90	4.15	0.01
Plankton nets	P90.200_Li	4.70	0.32
	P90.200_Hi	4.45	0.16
	P200_Li	4.08	1.00
	P200_Hi	3.93	0.08
Plankton nets + Looxster enrichment	L_P90.200_Li	4.78	0.15
	L_P90.200_H	4.50	0.36
	L_P200_Li	3.97	1.33
	L_P200_Hi	4.42	0.12

Supplementary Table S4 | Effect of prokaryotic DNA enrichment (by Looxster treatment) on the abundances of the 12 taxa selected as discriminant of the different size fractions. The selection of discriminant taxa is shown in Figure 2, and their relative abundances in Figure 3. The Looxster treatment can have different effect (i.e. overabundance or underabundance compared to the direct extraction samples) on the different size fractions. The "small fraction" and "large fraction" categories correspond to < 90 µm and > 90 µm fractions, respectively. These categories are based on the similarity of microbial community structure calculated by PERMANOVA (see main text). The adjusted p-value is obtained by Tukey HSD post-hoc test after ANOVA testing the interacting effect of Looxster * Size on each taxa.

Taxa	**Size Fraction with significant Looxster effect**	**Trend observed with Looxster**	**p adj**
Rhodobacteraceae	0.2 - 90 µm	Overabundance	0.00896
SAR11 clade	0.2 - 3 µm 0.2 - 90 µm > 0.2 µm	Underabundance	0.000128 0.002636 0.020302
Cyanobacteria	none	NA	NA
Oxalobacteraceae	none	NA	NA
Flavobacteriaceae	none (considering all fractions) small fraction (considering categories)	NA Underabundance	NA 0.0653530
Balneola	none	NA	NA
Puniceicoccaceae	none	NA	NA
Thioglobaceae	> 200 µm	Underabundance	0.00506
Halieaceae	none (considering all fractions) small fraction (considering categories)	NA Overabundance	NA 0.0012025
Actinobacteriota	none	NA	NA
Pirellulaceae	none	NA	NA
Magnetospiraceae	none	NA	NA

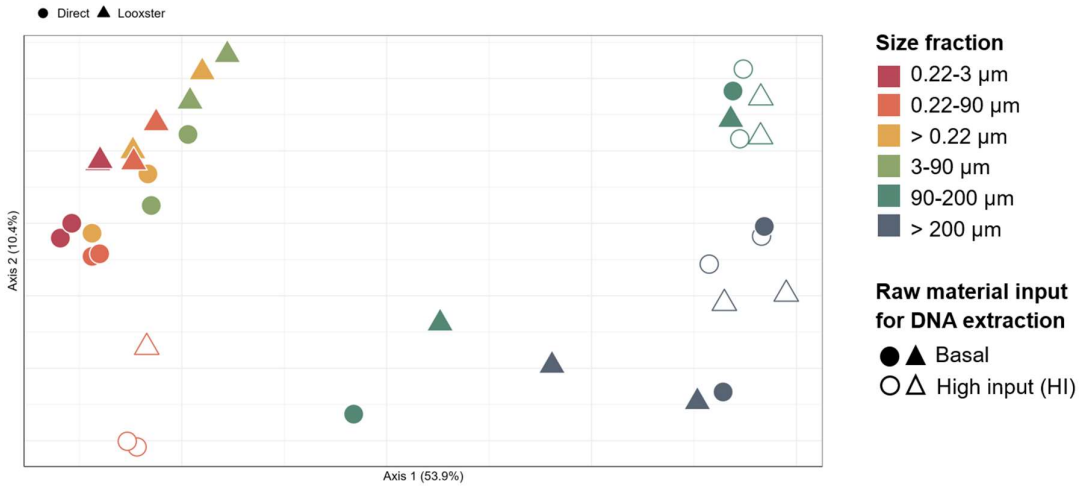

Supplementary Figure S1 | Community ordination without desorption samples by Principal Coordinate Analysis (PCoA) based on Bray Curtis dissimilarity index computed from the whole OTU abundance table. Samples are colored according to the planktonic size fraction. Symbol shapes indicate the DNA recovery methodology. Full and empty symbols represent samples obtained from, respectively, basal and high amount of raw material (water volume or plankton weight). The percentage of explained variance is indicated next to each axis.

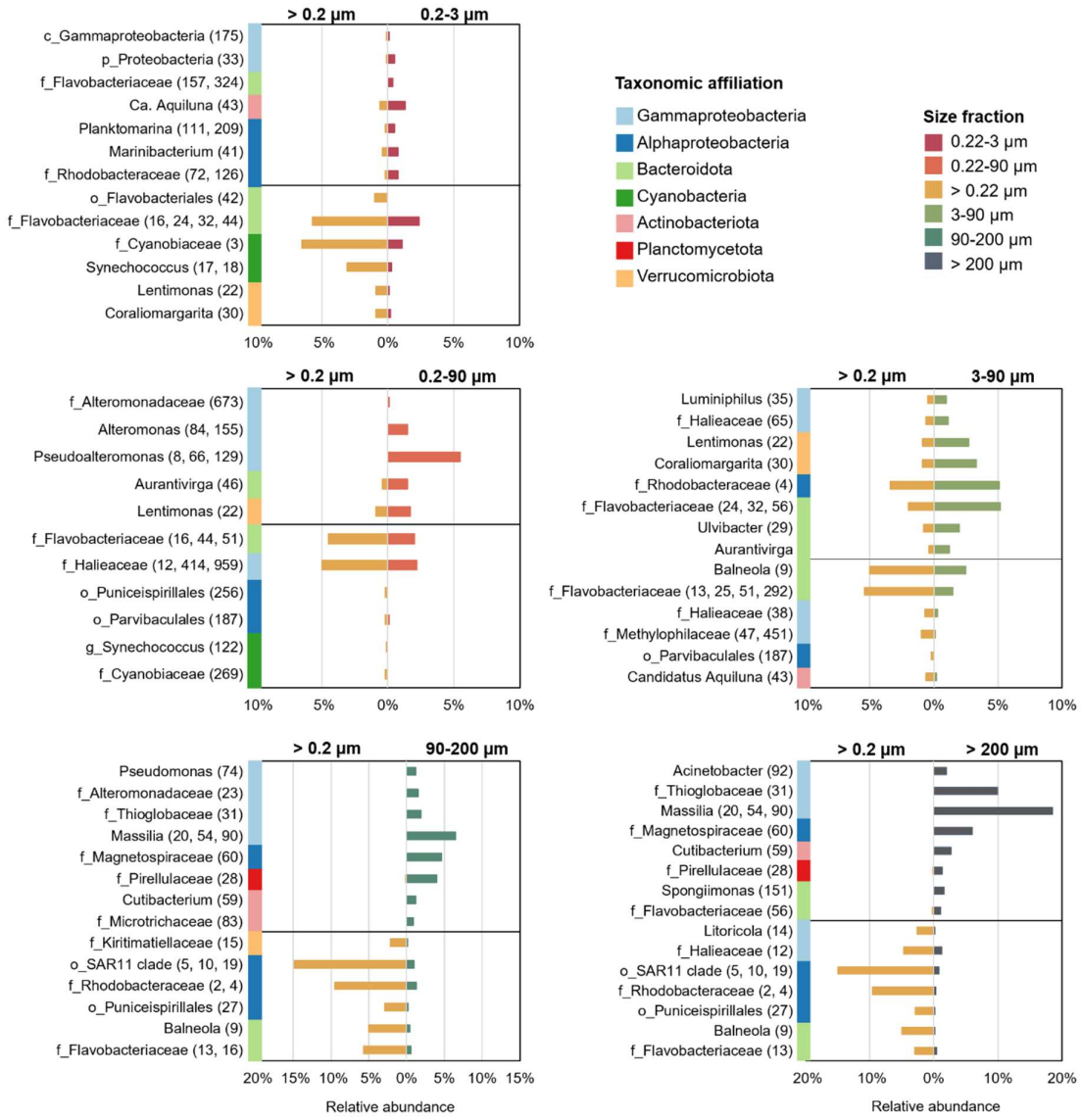

Supplementary Figure S2. Enrichment of specific taxa in the different size fractions compared to the bulk (> 0.2 µm) community. The 10 most significantly enriched taxa (p value < 0.05) obtained by pairwise LEFse analysis were agglomerated to the genus level (or at the last available taxonomic rank when genus affiliation is not available).

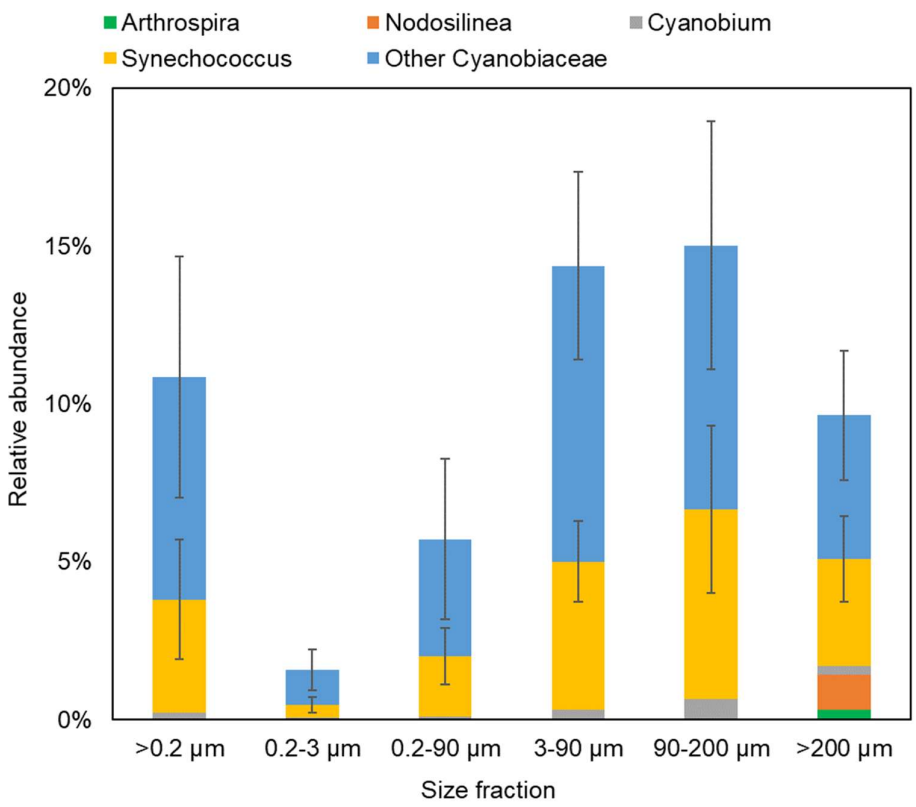

Supplementary Figure S3. Abundances of Cyanobacteria taxa among the different size fractions. Averages and standard deviations were calculated using all conditions excluding the desorption pre-treatment.

Additional references

Bokulich, N. A., Subramanian, S., Faith, J. J., Gevers, D., Gordon, J. I., Knight, R., ... & Caporaso, J. G. (2013). Quality-filtering vastly improves diversity estimates from Illumina amplicon sequencing. *Nature methods*, 10(1), 57-59.

Burke, C., Kjelleberg, S., & Thomas, T. (2009). Selective extraction of bacterial DNA from the surfaces of macroalgae. *Applied and environmental microbiology*, 75(1), 252-256.

Escudié, F., Auer, L., Bernard, M., Mariadassou, M., Cauquil, L., Vidal, K., ... & Pascal, G. (2018). FROGS: find, rapidly, OTUs with galaxy solution. *Bioinformatics*, 34(8), 1287-1294.

Mahé, F., Rognes, T., Quince, C., De Vargas, C., & Dunthorn, M. (2015). Swarm v2: highly-scalable and high-resolution amplicon clustering. *PeerJ*, 3, e1420.